



Opportunities and Challenges in Thermochemical Conversion of Municipal Solid Waste: A Comprehensive Review

March 2026

Changing the World's Energy Future

Nepu Saha, Russell Smith, Jordan Lee Klinger



DISCLAIMER

This information was prepared as an account of work sponsored by an agency of the U.S. Government. Neither the U.S. Government nor any agency thereof, nor any of their employees, makes any warranty, expressed or implied, or assumes any legal liability or responsibility for the accuracy, completeness, or usefulness, of any information, apparatus, product, or process disclosed, or represents that its use would not infringe privately owned rights. References herein to any specific commercial product, process, or service by trade name, trade mark, manufacturer, or otherwise, does not necessarily constitute or imply its endorsement, recommendation, or favoring by the U.S. Government or any agency thereof. The views and opinions of authors expressed herein do not necessarily state or reflect those of the U.S. Government or any agency thereof.

Opportunities and Challenges in Thermochemical Conversion of Municipal Solid Waste: A Comprehensive Review

Nepu Saha, Russell Smith, Jordan Lee Klinger

March 2026

**Idaho National Laboratory
Idaho Falls, Idaho 83415**

<http://www.inl.gov>

**Prepared for the
U.S. Department of Energy
Under DOE Idaho Operations Office
Contract DE-AC07-05ID14517**

1
2
3
4
5
6
7
8
9
10
11
12
13
14
15
16
17

**Opportunities and Challenges in Thermochemical Conversion of
Municipal Solid Waste: A Comprehensive Review**

Nepu Saha ^{a,*}, Russell C. Smith ^{a,†}, and Jordan Klinger ^a

^a Idaho National Laboratory, 1955 N. Fremont Avenue, Idaho Falls, ID 83415, USA

* Corresponding Author: email: nepu.saha@inl.gov, Tel: +1 208 526 4702

† This work was carried out during Russell Smith’s summer internship at Idaho National
Laboratory

18
19
20
21
22
23
24
25
26
27
28
29
30
31
32
33
34
35
36
37
38
39

Abstract

Recent advancements in thermochemical conversion processes have elucidated new pathways for converting municipal solid waste into valuable resources. This review explores the primary thermochemical conversion methods, including combustion, gasification, pyrolysis, torrefaction, hydrothermal carbonization, and hydrothermal liquefaction, emphasizing their potential roles in waste management and energy recovery. Key challenges including feedstock variability, ash behavior, and scale-up limitations are discussed alongside opportunities for hybrid systems and circular economy integration. A comparative analysis of research publications indicates a significant focus on thermochemical pathways within the broader context of municipal solid waste research, underscoring the growing interest in these technologies. Recent advancements in each thermochemical process, alongside their operational, technical, and economic challenges, are discussed. Comparative data reveal that torrefaction enhances the hydrophobicity and grindability of municipal solid waste components, though its energy densification benefits are more modest than those observed in biomass. Hydrothermal carbonization and liquefaction are highlighted for their ability to process high-moisture and heterogeneous waste streams. The review also synthesizes recent findings on reactor configurations, emissions control, and synergistic effects in co-processing municipal solid waste fractions. The findings underscore the importance of developing standardized protocols for municipal solid waste characterization and the need for innovative hybrid systems to improve efficiency.

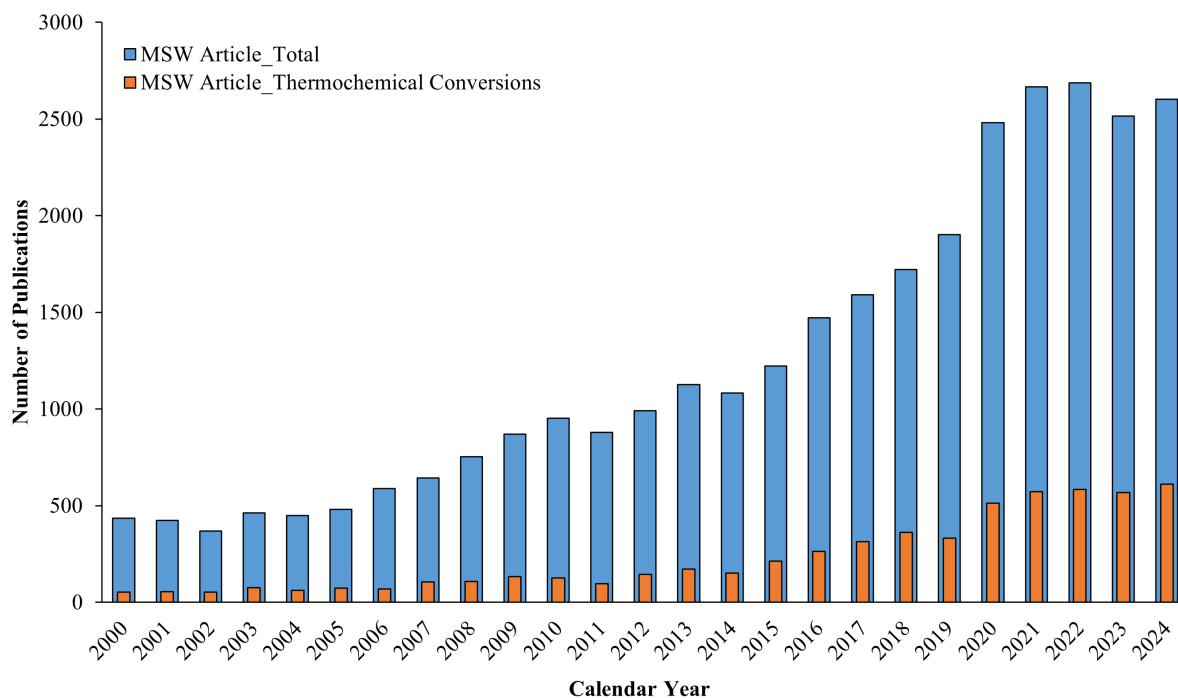
Keywords: Municipal solid waste; Feedstock variability; Thermochemical conversion; Waste-to-energy; Waste management.

40 **1 Introduction**

41 Municipal Solid Waste (MSW) management has evolved into a formidable challenge in the
42 contemporary urban landscape, driven by population growth, urbanization, and changing
43 consumption patterns. According to the United States Environment Protection Agency (US EPA),
44 292.4 million tons of MSW had been generated globally in 2018 which equivalent to 4.9 pounds
45 per person per day [1]. Out of 292.4 million tons, about 32.1% were recycled and composted, and
46 18.8% were combusted for energy recovery while the rest 50% were sent to landfill which releases
47 up to 193 million metric tons of carbon dioxide equivalent (MMTCO₂E) greenhouse gas to the
48 environment [1]. The escalating volumes of waste and resulting greenhouse gas emission
49 necessitate innovative and sustainable waste-to-energy (WtE) solutions. As the world grapples
50 with the pressing need to reduce reliance on finite fossil fuel resources and curb environmental
51 degradation, the role of MSW in the energy matrix gains prominence. Thermochemical conversion
52 processes, including pyrolysis, gasification, and combustion, have emerged as promising
53 technologies capable of transforming MSW into energy and value-added products. This review
54 examines the key thermochemical conversion pathways for MSW, with a focus on their potential
55 for energy and chemical recovery.

56 In recent years, the acceleration of research and technological developments in thermochemical
57 conversion has opened up new avenues for turning waste into a valuable resource. From producing
58 syngas for electricity generation to yielding biochar for soil improvement, thermochemical
59 conversion technologies hold the potential to redefine the utilization of MSW. However, the
60 journey from theoretical promise to practical implementation is fraught with challenges, ranging
61 from feedstock variability to stringent environmental regulations. Figure 1 presents a comparative
62 analysis of the total number of research publications related to MSW and those specifically

63 addressing thermochemical conversion of MSW. The data indicates that, proportionally, a
64 significant part of MSW-related research is concentrated on thermochemical pathways, suggesting
65 a growing interest in these technologies for waste valorization.



66
67 *Figure 1: Publications on MSW and thermochemical conversions of MSW since 2000. The “Web of Science” platform*
68 *was used to compile this list. The key words, such as torrefaction, pyrolysis, gasification, combustion, hydrothermal*
69 *carbonization and hydrothermal liquefaction were used for the thermochemical conversion related publications.*

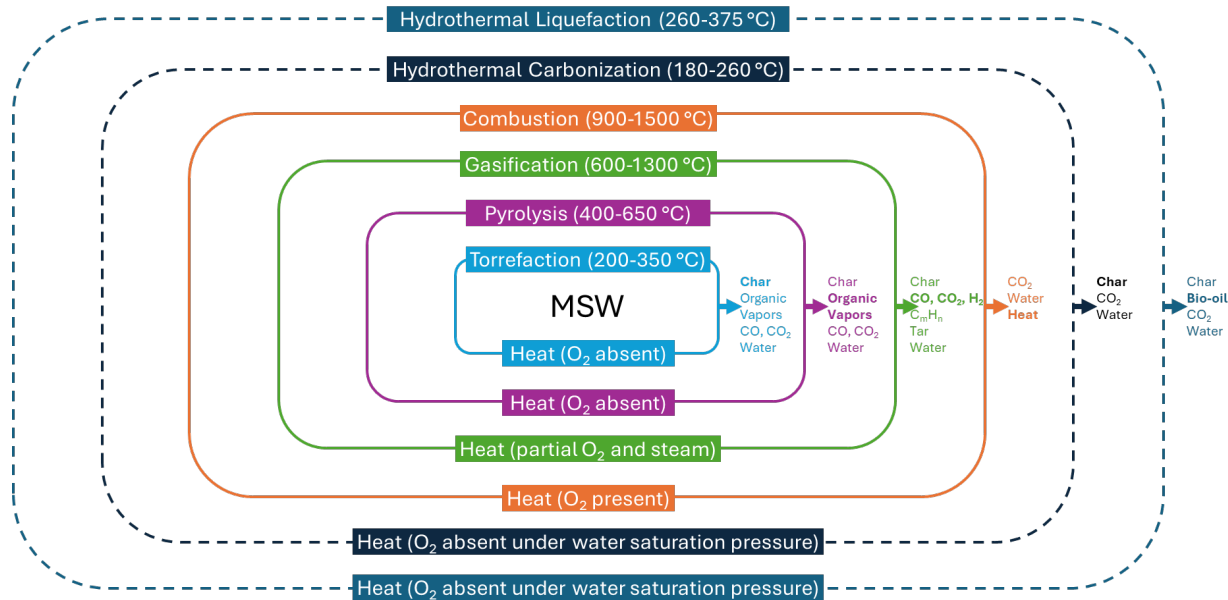
70 While numerous review articles have examined individual thermochemical pathways such as
71 pyrolysis or gasification, a comprehensive synthesis that integrates both dry and wet
72 thermochemical processes for MSW remains limited. Existing reviews often focus on specific
73 technologies or narrowly defined feedstocks, without addressing the interplay between feedstock
74 variability, preprocessing requirements, and hybrid system design. This review distinguishes itself
75 by (i) systematically comparing dry and wet thermochemical pathways under a unified framework,
76 (ii) emphasizing the role of MSW heterogeneity on process performance, and (iii) identifying
77 opportunities for integrating multiple conversion technologies to enhance efficiency and

78 circularity. It evaluates the technical and operational challenges that hinder the widespread
79 implementation of these technologies within waste-to-energy and waste-to-chemicals systems.
80 The analysis includes recent technological developments, environmental impacts, and relevant
81 economic and policy considerations. In the context of global efforts to achieve sustainability
82 targets, the assessment of thermochemical strategies for MSW treatment is increasingly relevant.
83 The following sections provide a detailed evaluation of the major thermochemical conversion
84 technologies, identify key opportunities and limitations, and outline the regulatory and societal
85 factors that influence their adoption. This review aims to offer a structured and evidence-based
86 reference for researchers, policymakers, and industry professionals engaged in advancing
87 thermochemical solutions for MSW valorization.

88 **2 Thermochemical conversion of MSW: opportunities and challenges**

89 Thermochemical conversion technologies encompass a diverse array of processes designed to
90 extract energy and produce chemicals from MSW. Generally, thermochemical conversions can be
91 categorized into two types: (i) dry conversions (*e.g.*, combustion, gasification, pyrolysis,
92 torrefaction) and (ii) wet conversions (*e.g.*, hydrothermal carbonization and liquefaction). Figure
93 2 illustrates the major differences among various thermochemical conversion processes regarding
94 operating conditions and conversion products. Although thermochemical processes such as
95 pyrolysis are often categorized based on dominant products (*e.g.*, carbonization vs. liquefaction),
96 hydrothermal processes are treated separately in this review due to their fundamentally different
97 reaction media and mechanisms. Hydrothermal carbonization and liquefaction occur in aqueous
98 environments under subcritical conditions, leading to distinct reaction pathways compared to dry
99 pyrolysis. Furthermore, hydrothermal carbonization predominantly yields solid hydrochar,
100 whereas hydrothermal liquefaction targets liquid biocrude production. This distinction is

101 particularly important for MSW, where high moisture content favors hydrothermal routes over
 102 conventional pyrolysis classifications.



103
 104 *Figure 2: Comparison of various thermochemical conversions with potential projects. The products mentioned in*
 105 *bold characters are the major product(s) from that specific process. The dashed line indicates the wet process*
 106 *while solid lines represent dry processes (figure modified from Matsakas, et al. [2]).*

107 2.1 Characteristics of MSW

108 MSW is a highly heterogeneous and complex feedstock composed of a wide range of organic and
 109 inorganic materials, including food waste, paper, plastics, yard waste, textiles, metals, glass, and
 110 inert residues [3]. The composition of MSW varies significantly depending on geographical
 111 location, socioeconomic conditions, seasonal variations, and waste management practices, making
 112 it inherently difficult to characterize and process consistently[3-7]. This variability directly
 113 impacts the performance, efficiency, and product distribution of thermochemical conversion
 114 technologies. Therefore, robust feedstock characterization and preprocessing strategies are
 115 essential to ensure consistent process performance.

116 The physical composition of MSW typically includes a large fraction of biodegradable materials
 117 (e.g., food and yard waste), along with recyclable components such as paper and plastics, and non-

118 combustible materials such as metals and glass. Studies have shown that organic fractions can
119 account for 30-60 wt% of MSW, while plastics and paper contribute significantly to the energy
120 content due to their higher carbon and hydrogen content[3, 4, 8]. The ultimate analysis of MSW
121 generally indicates carbon contents of 30-45 wt%, hydrogen 4-7 wt%, and oxygen 25-40 wt%,
122 reflecting its partially biogenic nature [4, 8]. Nitrogen and sulfur contents are typically low (<1
123 wt%), although they can vary depending on waste composition and influence emissions such as
124 NO_x and SO_x during thermochemical processing [9, 10].

125 Moisture content is one of the most critical parameters influencing MSW conversion. Depending
126 on the fraction of food and organic waste, moisture content can range from 20 to 60 wt% [6]. High
127 moisture content reduces the effective heating value and increases the energy required for drying,
128 thereby negatively affecting the efficiency of dry thermochemical processes such as combustion,
129 gasification, and pyrolysis. In contrast, wet thermochemical processes such as hydrothermal
130 carbonization and liquefaction are better suited for high-moisture feedstocks, as they utilize water
131 as a reaction medium.

132 The higher heating value (HHV) of MSW typically ranges from 6 to 20 MJ/kg, depending on the
133 relative proportions of combustible and non-combustible components [11]. Plastic-rich fractions
134 tend to exhibit higher HHVs due to their elevated carbon and hydrogen content, whereas food
135 waste and other oxygen-rich materials generally lower the overall energy density.

136 Ash content in MSW varies widely (typically 5-50 wt%) and is strongly influenced by the presence
137 of inorganic materials such as dirt, metals, glass, and mineral residues [3, 12]. The inorganic
138 fraction contains elements such as sodium, potassium, calcium, silicon, chlorine, and trace heavy
139 metals, which play a critical role in thermochemical processes. For example, alkali and alkaline
140 earth metals can promote slagging, fouling, and bed agglomeration in gasification and combustion

141 systems, while chlorine can lead to corrosion and the formation of hazardous compounds such as
142 HCl and dioxins [13-15]. The presence of heavy metals also raises environmental concerns related
143 to ash disposal and leachability, necessitating careful management and potential stabilization
144 treatments [16, 17].

145 The physicochemical characteristics of MSW strongly influence the selection and performance of
146 thermochemical conversion technologies. Dry processes such as combustion, gasification, and
147 pyrolysis require relatively low moisture content and benefit from higher energy density
148 feedstocks. In contrast, wet processes such as hydrothermal carbonization and liquefaction are
149 more suitable for high-moisture, organic-rich waste streams. Additionally, the heterogeneous
150 nature of MSW necessitates preprocessing steps such as sorting, size reduction, drying, and
151 blending to improve feedstock uniformity and enhance conversion efficiency [18, 19]. Thermal
152 pretreatment methods such as torrefaction and hydrothermal processing can further modify
153 feedstock properties, improving grindability, energy density, and reactivity [20, 21].

154 Overall, a comprehensive understanding of MSW characteristics is essential for designing efficient
155 and reliable thermochemical conversion systems. The following sections will elaborate on the
156 various thermochemical conversions of MSW.

157 **2.2 Dry processes**

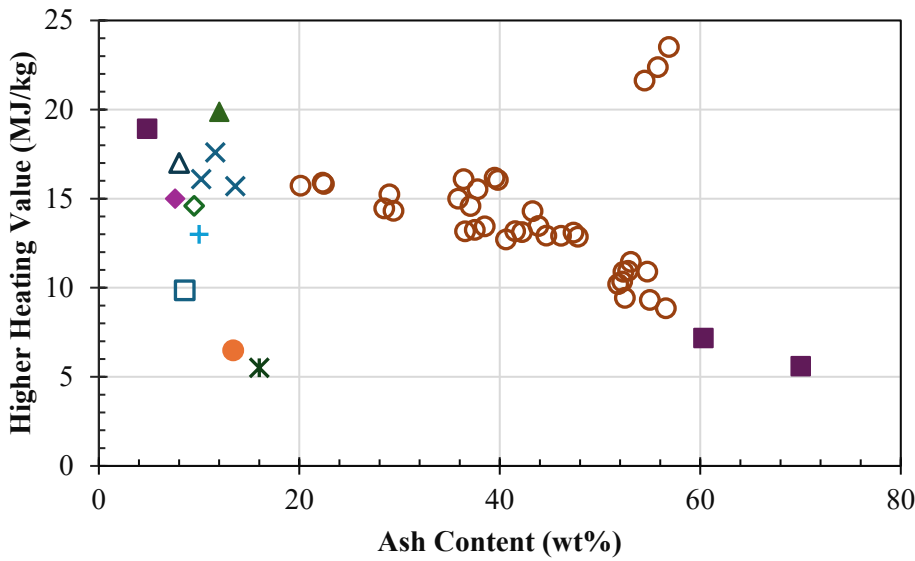
158 *2.2.1 Combustion*

159 Combustion, the most traditional form of WtE conversion, involves the direct burning of MSW to
160 generate heat and subsequently produce steam for electricity generation through turbines. It
161 remains the most established thermochemical conversion pathway for MSW worldwide,
162 particularly in urban areas where land is limited and waste volumes are high. The process not only
163 reduces the waste by mass about 70-80% and volume up to 90% but also generates useful energy

164 in the form of electricity and heat [22]. In modern WtE facilities, MSW is typically burned in
165 large-scale grate furnaces, which can handle heterogeneous feedstocks with little preprocessing
166 [23]. This robustness has contributed to the widespread deployment of incineration plants in
167 Europe, Japan, and parts of China [24].

168 For most of these facilities, the most important parameter for energy generation is the heating value
169 or energy density in the feedstock, which is largely dictated by the proportions of combustible and
170 non-combustible mass. Figure 3 illustrates an inverse relationship between ash content and HHV,
171 demonstrating why they are critically linked. Higher heating values reported in these studies range
172 from 6.3 to 19.1 MJ/kg [11]. Volatile matter content in MSW is also consistently high, typically
173 exceeding 59%, which supports rapid ignition and stable flame propagation [8]. Fixed carbon
174 values vary between 15% and 20%, providing sufficient energy density to sustain combustion
175 across staged chambers [12]. The ultimate analysis shows that carbon content generally falls
176 between 36% and 41%, hydrogen between 4.9% and 6.1%, and oxygen between 32% and 34%,
177 highlighting the semi-biogenic composition of MSW that includes food waste, paper, yard debris,
178 and plastics [25]. Nitrogen and sulfur contents remain relatively low, around 1.0% and below
179 0.5%, respectively, which is advantageous in mitigating NO_x and SO_x formation during
180 combustion [9]. Furthermore, seasonal variations in MSW composition have been shown to alter
181 proximate and ultimate analysis results, with food waste-rich streams yielding higher oxygen
182 content and lower HHVs, while plastic-rich fractions provide increased carbon and hydrogen
183 contents that improve energy recovery potential [6]. Comparative analyses have also highlighted
184 that the biogenic fraction of MSW contributes positively to renewable energy credits, making
185 combustion performance data critical for life-cycle assessment (LCA) of WtE systems [26, 27].
186 These values indicate that MSW, although less energy-dense than fossil fuels, is a viable feedstock

187 for heat and power generation when processed in optimized incineration systems. Other studies
188 have also emphasized that trace elements such as chlorine, potassium, and sodium, present in
189 varying amounts depending on regional waste composition, can influence slagging, fouling, and
190 corrosion tendencies in combustion systems [13, 14]. In addition, chlorine contents exceeding
191 0.3% have been correlated with enhanced formation of HCl and dioxins, which require additional
192 flue gas treatment steps [15].



193
194 *Figure 3: The relationship between ash content and higher heating value is illustrated using data compiled from*
195 *multiple literature sources [11, 12, 25, 28-34], with distinct markers denoting individual data sets from each*
196 *reference.*

197 Although technologies have been created and adapted to accommodate the heterogeneous nature
198 of MSW for combustion, most facilities are unique and inefficient due to the need to accommodate
199 a wide range of fuel properties, slagging and fouling discussed above, and overall thermal inertia
200 and energy transients in the plant [35]. These factors generally lead to a maximum thermal
201 efficiency of 65-70% even in ideal operation [35]. As a result of this, a significant portion of active
202 work in literature focuses on multi-phase modeling of combustion processes, particularly for grate-
203 fired and fluidized bed incinerators [36-44]. These studies use computational fluid dynamics

204 (CFD) simulations to model airflow, volatile release, char oxidation, and temperature profiles to
205 better understand, design, and optimize these combustion processes. Research by Wang *et al.* [45]
206 demonstrated how integrating radiative heat transfer models into CFD platforms can better predict
207 flame propagation and help redesign combustion chambers for temperature field flux influenced
208 by gas radiation. Similar efforts by McPhali *et al.* [46] aim to incorporate feedstock-specific data,
209 including proximate and ultimate analysis, into Aspen plus combustion models that calculate and
210 respond to changes in feedstock properties. Emerging studies are also exploring the co-combustion
211 of MSW with engineering fuels, such as hydrochar, biochar, coal, and refuse-derived fuel (RDF)
212 [47-50]. These co-firing strategies are being tested to address combustion inefficiencies associated
213 with low calorific value or high ash content in raw MSW. For instance, co-combustion with
214 hydrothermally treated MSW and coal has shown promising results decreasing polycyclic aromatic
215 hydrocarbons emissions compared to non-hydrothermally treated MSW as shown in work by Peng
216 *et al.* [48]. Additionally, the co-incineration of plastic-rich fractions is being actively studied for
217 both its energy contribution and its impact on synergy and ash residues [51]. Recent advancements
218 in process control and combustion efficiency have been achieved through the application of
219 numerical modeling and real-time control systems. Wu *et al.* [52] provide an in-depth analysis of
220 combustion simulation techniques, revealing how CFD models are used to optimize furnace
221 geometry, residence time, and air staging. These models allow plant operators to anticipate flame
222 instability, slagging, or incomplete combustion based on feedstock variability and adjust air
223 distribution accordingly [53]. In addition to conventional modeling approaches, Recent studies
224 have demonstrated the effectiveness of machine learning approaches for real-time prediction and
225 control of emissions in MSW combustion systems. For example, deep learning models such as
226 long short-term memory (LSTM) and hybrid neural networks have been successfully applied to

227 predict dioxin formation and NO_x emissions with high accuracy, enabling improved process
228 control under variable operating conditions [54, 55]. In addition, data-driven optimization
229 frameworks have shown the ability to adjust air distribution and key operating parameters
230 dynamically, resulting in enhanced combustion efficiency and reduced pollutant formation [56].
231 The integration of machine learning with combustion diagnostics further allows adaptive control
232 systems to maintain optimal combustion temperatures and reduce harmful emissions under varying
233 load conditions [56].

234 Another growing area of research is focused on combustion by-products, particularly bottom ash
235 and fly ash. The bottom ash produced from MSW combustion typically represents about 20% of
236 the input waste by mass and contains a mixture of glass, metals, ceramics, and mineral ash [57].
237 Depending on its composition, this ash can be used in construction applications such as road base
238 materials or concrete additives, provided it meets leachability and toxicity criteria [16]. Fly ash,
239 however, often contains higher concentrations of heavy metals and dioxins and is usually treated
240 as hazardous waste [42]. Li *et al.* [58] have explored methods to stabilize or vitrify fly ash to make
241 it safe for landfilling or recycling, including melting or sintering techniques that immobilize toxic
242 species. From a circular economy perspective, incineration has traditionally been criticized for its
243 “end-of-pipe” approach that seemingly conflicts with principles of material recovery. However,
244 recent strategies aim to integrate incineration into resource recovery loops. For example, metals
245 such as aluminum and iron are increasingly recovered from bottom ash via mechanical separation
246 [59]. Additionally, flue gas condensation systems enable heat recovery for district heating,
247 improving overall plant energy efficiency [60]. There is also growing interest in recovering
248 phosphorus and other critical materials from MSW combustion residues, especially as global
249 demand for fertilizers increases [61]. Studies now emphasize not only reducing their volume and

250 toxicity but also valorizing them as secondary resources [62-64]. Researchers are using analytical
251 techniques such as X-ray fluorescence (XRF), inductively coupled plasma mass spectrometry
252 (ICP-MS), and leaching tests to assess the suitability of ash for use in concrete, road base materials,
253 or as sources of critical elements such as zinc, aluminum, or rare earth metals [17, 63]. Recent
254 investigations are also evaluating ash aging and weathering behavior, recognizing that long-term
255 exposure to atmospheric CO₂ or water can alter ash mineralogy and leachability [17]. In parallel,
256 studies are optimizing vitrification and carbonation processes to stabilize hazardous fly ash and
257 enhance its environmental compatibility [65].

258 A critical research area in MSW combustion is emissions control. Modern incineration plants must
259 comply with stringent environmental regulations regarding the release of NO_x, SO_x, dioxins,
260 furans, and heavy metals [66]. Emission formation depends heavily on combustion temperature,
261 oxygen availability, and residence time [67]. For instance, excessive temperature spikes or poor
262 mixing can lead to incomplete combustion and formation of dioxins [68]. To counter this, many
263 facilities employ selective non-catalytic reduction (SNCR) or selective catalytic reduction (SCR)
264 systems for NO_x control, coupled with activated carbon injection and high-efficiency particulate
265 arresters (HEPA filters) to trap heavy metals and acid gases [69]. The development of smart
266 incinerators using sensor arrays and machine learning algorithms is gaining traction for regulatory
267 compliance and safe facility operation. These systems continuously monitor temperature, oxygen
268 levels, and flue gas composition to adjust fuel feeding rates and airflow in real time [70]. Rahat *et*
269 *al.* [70] have demonstrated that data-driven multi-objective combustion management systems can
270 significantly reduce NO_x emissions while improving boiler efficiency. Integrating such systems
271 can enable emissions traceability and regulatory compliance, as demonstrated in emerging pilot
272 projects across East Asia and the European Union [71, 72].

273 Oxy-fuel combustion has emerged as a promising enhancement to conventional incineration,
274 particularly in the context of carbon neutrality goals. In oxy-combustion, oxygen replaces air as
275 the oxidizer, producing flue gas stream composed primarily of CO₂ and water vapor, which is
276 conducive to post-combustion carbon capture [73]. Becidan *et al.* [74] demonstrated that oxy-fuel
277 combustion of MSW does not significantly compromise combustion efficiency and can be
278 integrated into BECCS (bioenergy with carbon capture and storage) systems. This has important
279 implications for MSW management, especially given that over 50% of typical MSW is biogenic
280 in origin, enabling negative carbon emissions [75].

281 Public perception and policy also play a significant role in the development and deployment of
282 MSW combustion technologies. In many regions, incineration faces public resistance due to
283 concerns over health risks and emissions, even though modern plants operate well within
284 regulatory limits [76]. Transparent monitoring, community engagement, and investment in state-
285 of-the-art emissions control technologies are essential to overcoming these barriers. Policy
286 developments such as carbon pricing, renewable energy incentives, and landfill taxes can help
287 level the playing field between incineration and other waste treatment options.

288 2.2.2 *Gasification*

289 Gasification is a thermochemical process that transforms carbonaceous materials into a syngas
290 (synthesis gas) consisting of CO, H₂, and CH₄ along with other low-molecular-weight
291 hydrocarbons. The products may also contain several undesired components such as particulate
292 matter, tar, alkali metals, chlorine, and sulfide depending on the feedstock quality [77]. The process
293 occurs at high temperatures, typically exceeding 700 °C, and involves a controlled reaction with a
294 limited oxygen supply.

295 Fixed bed gasifiers, including updraft and downdraft configurations, are among the earliest
296 gasification systems adapted for MSW. These systems are characterized by a relatively simple
297 design and operation, making them suitable for small-scale or decentralized applications.
298 However, they are limited by feedstock heterogeneity and are prone to tar formation, particularly
299 in updraft systems. Downdraft gasifiers, while producing cleaner syngas, require more uniform
300 feedstock and are sensitive to moisture content, which is a common challenge with MSW. On the
301 other hand, fluidized bed gasifiers, both bubbling and circulating types, offer improved feedstock
302 flexibility and better temperature uniformity due to enhanced mixing. These systems are well-
303 suited for MSW, which is often heterogeneous and contains varying moisture levels. Fluidized
304 beds can accommodate a wide range of particle sizes and compositions, making them attractive
305 for large-scale WtE applications.

306 Entrained flow gasifier, traditionally used for coal, operates at higher temperatures (1200-1600 °C)
307 and require finely pulverized feedstock. Using MSW in entrained flow gasifiers is gaining interest
308 due to their high carbon conversion efficiency and low tar output. However, even after extensive
309 pre-treatment, the MSW may not meet the quality to feed into the entrained flow gasifier. In recent
310 years, plasma gasification showed the capability of handling highly heterogeneous and hazardous
311 MSW streams. By generating extremely high temperatures (>3000 °C) using plasma torches, this
312 technology ensures complete breakdown of organic matter and vitrification of inorganic residues
313 [78]. Recent reviews have highlighted advancements in plasma torch design, reactor
314 configurations, and system integration, leading to improved process efficiency and syngas
315 production [79, 80]. In addition, plasma-assisted reforming has been shown to effectively reduce
316 tar formation through the generation of reactive species such as OH and O radicals, enhancing
317 syngas cleanliness and downstream usability [81]. Modeling and experimental studies further

318 demonstrate that plasma gasification can achieve high syngas yields and improved carbon
319 conversion efficiency through optimization of operating parameters and gasifying agents [82].
320 Despite these advantages, challenges related to high energy demand, capital cost, and system
321 scalability remain key barriers to widespread commercialization [78].

322 Different components of MSW, including organic materials like food waste, and inorganic
323 materials such as plastics and metals, possess unique gasification characteristics. For instance,
324 Xiao *et al.* [83] reported that biomass components, such as paper and wood, yield high quality
325 syngas due to their favorable chemical structures for gasification. In contrast, materials like waste
326 plastics offer higher gas yields due to their high carbon and hydrogen content, but the resulting
327 syngas can be of lower quality if contaminants from additives or incomplete conversion are
328 present. Kitchen waste, often rich in moisture and organic content, typically exhibits the lowest
329 gasification performance, resulting in lower syngas yields and heating values. This variability
330 necessitates tailored gasification strategies to optimize syngas production based on the specific
331 composition of the waste being processed. Gasification temperature is a critical factor affecting
332 syngas composition and yield. As the temperature increases, it promotes several key reactions that
333 enhance gas production, including the Boudouard reaction, steam methane reforming, and the
334 water-gas shift reaction [84]. For instance, studies have shown that raising the temperature from
335 700 °C to 900 °C can significantly increase the production of H₂ and CO [85]. Higher gasification
336 temperatures facilitate the breakdown of complex organic molecules and promote secondary
337 reactions that yield more valuable gas products. However, temperatures exceeding 900 °C can lead
338 to a decrease in H₂ production due to competing reactions that favor CO formation, highlighting
339 the delicate balance required in gasification temperature management [84]. The choice of
340 gasification medium, such as air, steam, or CO₂ plays a significant role in determining the quality

341 and composition of the produced syngas [86]. Air gasification typically leads to lower heating
342 values (LHV) of syngas in the range of 4 to 7 MJ/m³, primarily due to the dilution effect of nitrogen
343 present in the air [87, 88]. Conversely, steam gasification tends to yield hydrogen-rich syngas,
344 achieving syngas LHVs between 8 and 12 MJ/m³ [89]. The steam-to-MSW ratio is crucial, as
345 optimal ratios enhance syngas production by promoting steam reforming reactions. Research
346 suggests that an increase in steam-to-MSW ratio correlates with higher concentrations of H₂ and
347 CO, while excessive steam can inadvertently lower system temperatures and reduce overall
348 gasification efficiency. Studies have also shown that the addition of steam can improve carbon
349 conversion efficiency by facilitating the reactions necessary for syngas production [90].

350 The oxidant-to-MSW ratio is identified a key parameter in gasification that influences the partial
351 combustion of waste and the resulting syngas composition [91-93]. An optimal oxidant-to-MSW
352 ratio typically falls within the range of 0.1 to 0.4 for air gasification, balancing the combustion and
353 gasification reactions to maximize syngas yield while minimizing the production of unwanted by-
354 products [84]. Studies indicate that maintaining an optimal oxidant-to-MSW ratio can enhance the
355 overall carbon conversion efficiency [91]. However, as the oxidant ratio increases, it can lead to a
356 rise in combustion reactions at the expense of syngas quality, necessitating careful monitoring and
357 adjustment of the oxidant-to-MSW ratio to ensure efficient gasification. Zheng *et al.* [91] reported
358 that maintaining a carbon dioxide-to-MSW ratio around 0.83 during CO₂ gasification improve
359 syngas yield by promoting the thermal cracking of char, thereby increasing the overall efficiency
360 of the gasification process.

361 In addition to temperature and oxidant ratios, reactor configuration exerts a strong influence on tar
362 levels, carbon conversion, and syngas quality. Fixed-bed (updraft/downdraft) systems are
363 mechanically simple and suited for smaller scales but can exhibit higher tar unless operated at

364 elevated temperatures or with downstream cracking [94-97]. Bubbling and circulating fluidized
365 beds provide superior mixing and heat transfer, enabling more uniform temperatures, lower tar,
366 and higher cold gas efficiency across heterogenous MSW feeds [98, 99]. Entrained flow gasifiers
367 including plasma-assisted designs can achieve very low tar and high carbon conversion at ≥ 1200
368 $^{\circ}\text{C}$ with fine feed sizes, at the expense of higher O_2 or energy demand and tighter feed preparation
369 requirements [100-102]. Catalytic and sorbent-assisted routes are increasingly reported to suppress
370 tar and tune syngas properties. Natural olivine and calcined dolomite crack tars and capture alkali
371 or chlorine species, while Ni-based catalysts often supported on Al_2O_3 , MgAl_2O_4 , or $\text{CeO}_2\text{-ZrO}_2$
372 drive steam and shift reactions to elevate H_2 yield. Deactivation via sulfur/chlorine/alkali
373 poisoning can be mitigated using guard beds or periodic regeneration [103-106]. Active-bed
374 additives such as CaO can capture CO_2 in sorption-enhanced gasification, increasing apparent H_2
375 concentration and improving cold gas efficiency under steam-rich conditions [107].

376 Table 1 demonstrates the combined influence of feedstock composition and gasifier configuration
377 on syngas quality, tar formation, and solid residue yields in MSW gasification. Updraft fixed-bed
378 gasifiers operating at 800°C with plastic packaging mixture (PPM), solid recovered fuel (SRF),
379 and waste fraction after drum separator sorting (FDS) MSW streams produce comparable specific
380 syngas yields; however, they exhibit lower H_2/CO ratios and tar yields that vary with feedstock
381 characteristics. Notably, FDS generates more char due to its higher ash and fines content. In
382 contrast, downdraft gasifiers operated at 1000°C with engineered blend pellets of paper-mill
383 rejects sourced from two different mills, such as newsprint mill (AN) and brown paper mill (SSK),
384 along with de-inking sludge, and wood chips showed higher gas yield, elevated H_2/CO ratios, and
385 reduced tar content, underscoring the advantages of fiber-rich MSW streams. Plasma moving-bed
386 and bubbling fluidized-bed systems treating unsorted MSW further illustrate that increased

387 operating temperatures and enhanced mixing intensities can elevate the H₂/CO ratio, even though
 388 at the expense of higher energy input and, in some cases, increased char production. These
 389 observations reinforce the conclusion that both feedstock fractionation and reactor design must be
 390 co-optimized to achieve desired syngas quality and minimize undesirable by-products. This aligns
 391 with findings from Gao et al. [108], who emphasize that feedstock properties (e.g., ash and volatile
 392 content), gasifier type, and operating conditions (temperature, equivalence ratio) collectively
 393 determine syngas composition and conversion efficiency in biomass and MSW gasification
 394 systems.

395 *Table 1: An overview of MSW gasification in various gasifiers. NR indicates “not reported” in the literature.*

Gasifier type	Operating temperature (°C)	Feedstock	Equivalence ratio	Product (wt%)			Syngas quality (H ₂ /CO)	Ref.
				Gas	Tar	Char		
Fixed-bed updraft	800	PPM	0.15	94.48	2.76	2.76	1.32	[96]
			0.21	95.81	1.86	2.33	1.02	
		SRF	0.15	86.25	3.50	10.25	0.49	
			0.21	88.87	2.83	8.30	0.56	
			FDS	0.15	73.17	1.61	25.23	
0.21	81.97	1.08		16.96	0.50			
Fixed-bed downdraft	853	Refuse-derived fuel	0.30	NR	NR	NR	0.92	[109]
	918	MSW	0.40	NR	NR	NR	0.57	[110]
	1090	Mixed MSW	0.35	NR	NR	NR	1.11	[111]
Fixed-bed downdraft	1000	20% AN reject pellets, 80% wood chips	0.36	98.72	0.43	0.85	0.66	[112]
			0.53	97.82	0.22	1.96	0.59	
		15% AN reject pellets, 20% de-inking sludge, 65% wood chips	0.36	96.01	0.50	3.49	0.61	
			0.27	89.25	0.19	10.56	0.53	
		20% SSK reject pellets, 80% wood chips	0.28	98.98	0.25	0.76	0.58	
			0.24	98.27	0.10	1.63	0.51	
		70% SSK reject pellets, 30% wood chips	0.34	97.90	0.56	1.55	0.68	
			0.22	96.50	0.64	2.86	0.70	
Plasma moving-bed updraft	1000-1200	MSW+plastics	NR	~85	<1.0	~10-15	1.0-1.2	[78]
Bubbling fluidized bed	400-700	Mixed MSW	0.25-0.35	80-90	2-5	5-15	1.78 (steam), 0.64 (CO ₂)	[113]
Entrained flow	1200-1500	MSW, refuse-derived fuel	0.25-0.35	>90.0	<1.0	<5.0	1.0-1.5	[84]

396

397 Despite these advancements, challenges remain in managing ash chemistry, mitigating corrosion
398 and fouling, and ensuring consistent syngas quality from variable MSW feedstocks. For example,
399 moisture contents greater than 25-30 wt% typically depress reactor temperature, raising tar
400 formation, and decreasing H₂/CO production. Hence, feedstock pre-conditioning plays a
401 significant role in gasification operability. Drying or mild torrefaction 200-300 °C can remedy this
402 while also improving grindability, reducing O/C ratio, and stabilizes feed quality [18, 114]. In
403 addition, mechanical preprocessing focusing on size classification and removal of inert or metals
404 enhances gasifier throughput and reduces bed agglomeration risks in fluidized beds [19]. Beyond
405 air or steam, CO₂ as a gasifying agent, dry reforming, or Boudouard pathways can upgrade plastic-
406 rich fractions, while co-gasification with biomass, sewage sludge, or paper rejects can balance H/C
407 ratios and ash behavior. Several studies show synergistic effects that reduce tar and raise H₂/CO
408 at optimized blend ratios [115-118]. Pressure up to 30-60 bars can facilitate downstream synthesis
409 of methanol, though it may increase methane formation and impose stricter tar control because it
410 can foul the equipment and poison the catalyst [119, 120]. Ash chemistry such as alkali, chlorine,
411 silica, and metals governs slagging, fouling, and bed agglomeration. High K/Na with silica can
412 form low-melting silicates, with mitigation strategies including bed material selection (i.e.,
413 bauxite, olivine), temperature windows avoiding sticky phases, and upstream removal of fines and
414 glassy fractions [121-123]. In chlorine-bearing MSW, volatilization of alkali chlorides contributes
415 to corrosion and particulate emissions; sorbents such as kaolin and limestone optimize quench and
416 cleanup to reduce these risks [124].

417 Tar formation remains a significant challenge, potentially leading to blocking, fouling, and
418 corrosion [2]. Various methods exist for tar removal, including physical processes like filters,
419 scrubbers, and wet electrostatic precipitators, and chemical processes such as thermal and catalytic

420 cracking. Hu *et al.* [108] found that tar can be completely decomposed at elevated temperatures of
421 950 °C. Recent advancements in steam gasification show promise for high hydrogen yield with
422 reduced tar formation. He *et al.* [109] observed that steam gasification at 850-950 °C in the
423 presence of a calcined dolomite catalyst can completely decompose tar. Different gasifier types
424 also influence tar formation, with entrained flow gasifiers demonstrating reduced tar production
425 due to their higher operating temperatures compared to fluidized bed and fixed bed gasifiers [110-
426 112]. However, feeding non-traditional feedstocks into entrained flow gasifiers presents its own
427 set of challenges.

428 The advantages of MSW gasification over combustion include the potential to produce syngas,
429 which can be utilized in conventional burners. However, syngas may contain particulate matter,
430 acid gases, and organic pollutants due to the heterogeneous and contaminated nature of MSW (*e.g.*,
431 halogenated plastics, glass, dirt). The costs associated with cleaning gasification-derived syngas
432 may exceed those of incineration, which limits the commercial availability of MSW gasification
433 plants in the United States [104]. Additionally, the composition variability of MSW, which can
434 differ regionally and seasonally, impacts both the gasification efficiency and syngas quality [105].
435 Robust pre-treatment processes, including mechanical sorting, shredding, and blending, can
436 enhance feedstock homogeneity, thereby improving gasification efficiency. Effective emission
437 control technologies, such as electrostatic precipitators and scrubbers, are crucial for capturing
438 harmful pollutants like particulate matter, dioxins, and heavy metal.

439 Integrating gasification with advanced cleanup systems and downstream synthesis processes
440 underscores its potential in circular economy frameworks, but economic and scale-up hurdles
441 persist. Recent advancements in gasification have incorporated machine learning and data-driven
442 techniques to optimize process parameters, predict syngas composition, and manage operational

443 variability associated with heterogeneous MSW feedstocks [56, 108]. These tools facilitate
444 improved control over key variables such as temperature, equivalence ratio, and gasifying agent
445 selection, leading to enhanced syngas quality and overall process efficiency [90, 108]. The
446 adoption of such digital optimization strategies represents a growing trend toward more intelligent
447 and adaptive thermochemical conversion systems. Ongoing research into co-gasification
448 strategies, pressure effects, and digital optimization tools (*e.g.*, CFD, machine learning) will be
449 essential for improving efficiency and enabling broader deployment of MSW gasification as a
450 sustainable WtE technology.

451 2.2.3 Pyrolysis

452 Pyrolysis involves the thermal decomposition of organic materials in the absence of oxygen,
453 resulting in the production of three primary products, such as char, liquid bio-oil, and gases. The
454 process operates at moderate temperatures, typically between 400 and 800 °C, promoting the
455 breakdown of complex polymers into simpler, energy-rich compounds.

456 Lu *et al.* [125] recently compiled many literature sources concerning slow pyrolysis of MSW [126-
457 133]. Their review looked at pyrolysis of many feedstock including plastics (Polyethylene (PE),
458 Polypropylene (PP), Polystyrene (PS), Polyethylene terephthalate (PET)), paper and cardboard
459 (office paper, newspaper, corrugated cardboard, mixed paper products), wood and woody biomass
460 (woodchips, sawdust, branches and twigs, forestry residues), food and organic wastes (food scraps,
461 vegetable peels, fruit waste, expired food products), yard and green waste (grass clippings, leaves,
462 tree trimmings, garden waste), agricultural residues (straw, corn stover, rice husks, wheat husks),
463 mixed MSW (household waste (after sorting and pre-treatment), municipal solid waste streams,
464 mixed recyclables), and specialty organic wastes (rubber (*e.g.*, tires), textile waste (natural fibers),
465 sewage sludge, industrial organic waste (*e.g.*, food processing waste)). While each feedstock/study

466 has unique and valuable findings, these diversity of feed materials used in MSW pyrolysis can be
467 grouped into several categories based on common compositions, yield patterns, waste quality
468 improvements, and beneficial end uses. High carbon content feed materials like plastics and
469 rubber, along with high cellulosic content materials such as paper, cardboard, and woody biomass,
470 exhibit similar compositions, leading to high yields of bio-oil and syngas. On the other hand,
471 organic-rich materials such as food waste, yard waste, and green waste typically produce
472 substantial amounts of biochar, which can be used for soil amendment and carbon sequestration.
473 Mixed organic and inorganic content feeds like municipal sludge and industrial organic waste,
474 after sorting and contaminant removal, provide a balanced yield and contribute to waste volume
475 reduction and material recycling. Homogenized and dried waste streams such as shredded mixed
476 MSW, dried food waste, and dried yard waste are often pre-treated to achieve uniformity and
477 moisture reduction, enhancing pyrolysis efficiency. These feed materials, along with sorted
478 plastics and paper, tend to produce balanced yields of bio-oil, syngas, and biochar, making them
479 versatile for energy production, chemical feedstocks, and waste minimization.

480 Different feed materials for MSW pyrolysis can be grouped based on their compositional makeup,
481 such as carbon, hydrogen, and oxygen content, carbohydrate concentration, etc. to reflect feedstock
482 quality similarities. These similarities influence the pyrolysis process and the types of products
483 generated. High carbon content materials include plastics like PE and PP, rubber (*e.g.*, tires), and
484 coal-derived products. Feed materials with high cellulosic content encompass paper and cardboard,
485 wood and woody biomass such as wood chips and sawdust, and agricultural residues like straw
486 and husks. High moisture and organic content feed materials are typically food waste, yard waste
487 including grass clippings and leaves, and green waste such as vegetable scraps and garden waste.
488 Mixed organic and inorganic content materials include mixed MSW after sorting, municipal

489 sludge, and industrial organic waste. High lignin content materials consist of woody biomass like
490 wood chips and branches, agricultural residues with high lignin content such as corn stover and
491 rice husks, as well as bark and forestry residues.

492 Though yields can vary depending on specific feed characteristics and pyrolysis conditions like
493 temperature and residence time, feedstock qualities often lead to similar pyrolysis yield patterns
494 of products (bio-oil, syngas, and biochar) derived from pyrolysis. For instance, feed materials that
495 typically produce high bio-oil (liquid) yields include plastics such as PE and PP, rubber materials
496 like tires, and certain types of biomass such as wood chips and sawdust. Materials that yield a high
497 amount of syngas include mixed MSW with a high proportion of organic waste, food waste, and
498 agricultural residues like corn stover and rice husks. High biochar yields are commonly associated
499 with woody biomass such as wood chips and branches, agricultural residues like straw and husks,
500 and yard waste including leaves and grass clippings, derived from higher fixed carbon contents.
501 Some feed materials produce a balanced yield of bio-oil, syngas, and biochar, such as mixed
502 organic waste, paper and cardboard, and certain combinations of plastics and organic materials.

503 The diverse material fractions in MSW lead to a variety of beneficial uses for MSW pyrolysis,
504 optimizing waste management and resource recovery. Different feed materials used in MSW
505 pyrolysis can be grouped based on their beneficial end uses. For energy production, feed materials
506 such as mixed MSW (after sorting and pre-treatment), plastics like PET and High-density
507 polyethylene (HDPE), paper and cardboard, yard waste including grass clippings and leaves, and
508 food waste are commonly used. These materials are optimized to produce bio-oil, syngas, or
509 biochar, which can be used as fuel or energy sources. As chemical feedstocks, plastics such as PET
510 and HDPE can produce valuable chemicals like hydrocarbons and monomers, while wood and
511 yard waste can yield chemicals like acetic acid and methanol. Paper and cardboard can also be

512 converted into valuable chemicals such as furans and levoglucosan through pyrolysis. For soil
513 amendment purposes, organic waste including food waste and yard waste, as well as agricultural
514 residues like straw and husks, are used to produce biochar, which enhances soil quality and
515 sequesters carbon. In terms of waste minimization and recycling, mixed MSW can significantly
516 reduce overall waste volume and allow for the recovery of metals. Plastics can be processed to
517 reduce plastic waste and recover monomers or hydrocarbons, while paper and cardboard can be
518 recycled to reduce waste and recover fibers.

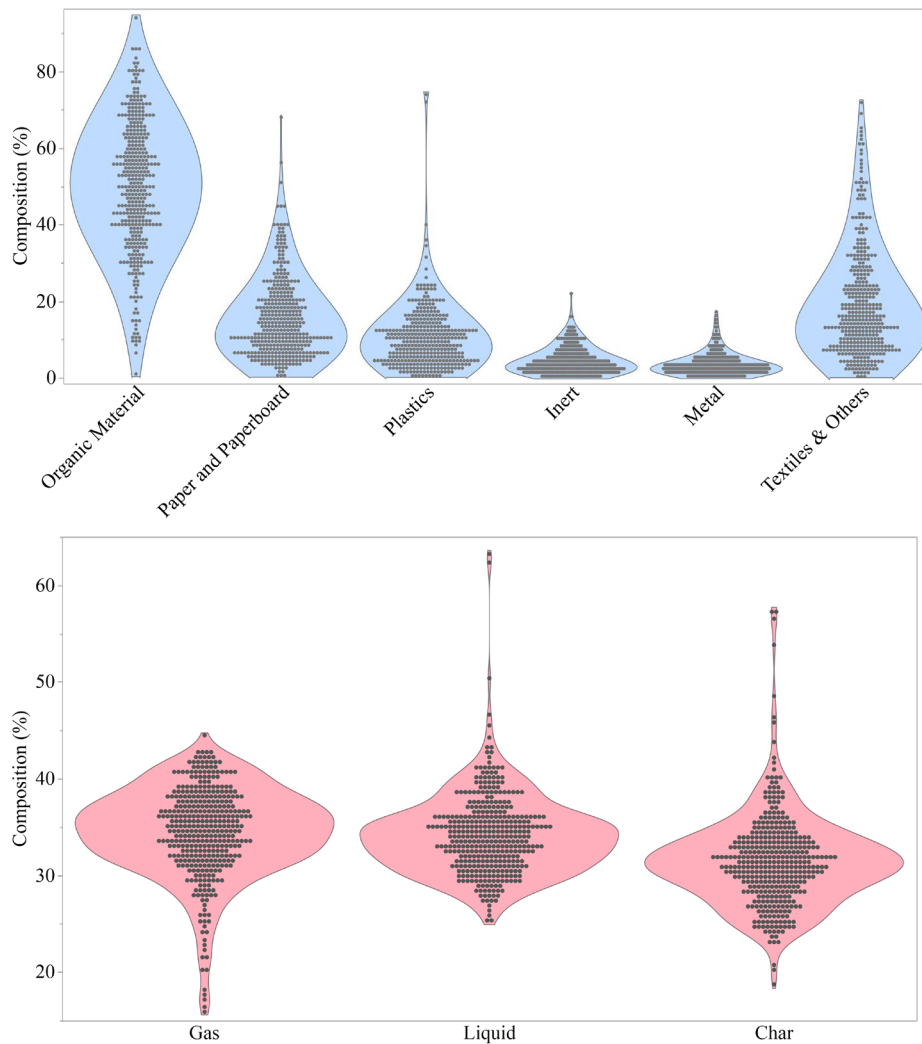
519 Due to the complex nature of MSW as a mixture, it is perhaps unsurprising that different samples
520 of MSW as well as the various components and their mixtures can behave very differently during
521 pyrolysis. Synergistic co-pyrolysis involves the interaction of various MSW components during
522 pyrolysis, which can significantly impact reaction rates and product yields. When different
523 constituents are combined during pyrolysis, complex reactions between the intermediates can lead
524 to synergistic effects that alter the rate of pyrolysis and the quantity and quality of the end products.
525 For example, co-pyrolyzing food waste with other MSW components like lignocellulosic materials
526 can accelerate pyrolysis rates and alter product distributions. The presence of excess oxygen in
527 food waste typically results in pyrolysis oils with high oxygenate levels but combining it with low
528 oxygen/carbon (O/C) ratio materials can improve the quality of the oils. For example, Chen *et al.*
529 [134] noted a more than double increase in hydrocarbon olefin production for comingled food
530 waste and tires. Co-pyrolysis of food waste with lignocellulosic materials can lead to increased
531 hydrocarbon production and reduced non-hydrocarbon content [135]. Furthermore, combining
532 food waste with algae biomass can increase gas yield while reducing oil yield but improve the
533 heating value of the oil [136].

534 Plastic waste, characterized by high carbon and hydrogen content and negligible oxygen content,
535 also exhibits significant synergistic effects during co-pyrolysis with other MSW constituents. For
536 instance, co-pyrolyzing plastic waste with biomass [137] can enhance oil yield and improve its
537 heating value. Different plastics exhibit varying interactions with biomass, with some
538 combinations promoting hydrocarbon production [138] and others influencing char formation
539 [139, 140].

540 Biomass waste, consisting of cellulose, hemicellulose, and lignin, shows diverse thermal
541 degradation behaviors [141, 142]. Co-pyrolysis of biomass with plastics or other organic materials
542 can shift product distribution from char to pyrolysis oil and syngas. For instance, co-pyrolyzing
543 biomass with short-chain organic compounds can increase oil and syngas yields, while lignin
544 presence can enhance product quality under certain conditions [143].

545 Other review articles discussing the pyrolysis of MSW and components have documented
546 additional insights and applicability in various regions around the globe [7, 144]. For example, Du
547 *et al.* [7] reviewed waste compositions from cities in eastern China in addition to Tokyo,
548 Singapore, Berlin, and MSW that could be excavated from long-standing landfills from China,
549 Sweeden, Belgium, Australia, Thailand, Estonia, Finland, and India. In general, it was concluded
550 that legacy wastes had much different composition than landfill inbound waste, primarily due to
551 the decay and loss of organics. Most locations reported plastic, rubber, and stones/aggregate to be
552 major contributing factors in landfill resources. Wood and paper still existed in larger quantities in
553 Finland, as well as site specific locations in Sweeden and Austria, with larger proportions of wood.
554 Thailand, China, and Estonia also had notable fraction of glass. For these minable resources, the
555 largest fraction (39-71%) was attributed to ‘fines’, or otherwise small, undefined/undefinable
556 fractions, highlight the lack of definition and understanding that yet remains about these resources.

557 Other studies form additional insight for a more comprehensive global view of MSW compositions
558 [4, 5]. Based on average pyrolysis performance data reported in [125, 128, 132, 145-151], and
559 using location-based compositional data from [4, 7, 152], a summary of MSW compositions and
560 expected pyrolysis results are presented in Figure 4. Although few if any distinct trends can be
561 noted from this wealth of data, there is ample indication that their processes such as pyrolysis can
562 take advantage of these resources around the globe. In addition, the wide scatter in waste fractions
563 and resulting yields indicate that future work in the area of waste sortation, processing, and
564 upgrading could significantly improve the performance and uniformity of MSW pyrolysis.



565 *Figure 4: Variability of components in MSW (top) along with their impact in product yields (bottom).*

566 Many proposed technologies and reactor styles for pyrolysis of MSW have been recently
567 summarized [153]. At the forefront of these technologies are different types of reactors. Fixed-bed
568 reactors, while commonly used in laboratory settings, exhibit low heat transfer efficiency and are
569 not suitable for large-scale applications due to their poor heat distribution and lengthy processing
570 times [154]. In contrast, rotary kiln reactors are more prevalent in industrial settings. They facilitate
571 good mixing of waste and allow for flexible adjustments in residence time, though they still operate
572 under slower heating rates, resulting in significant char production. For example, Li *et al.* [155]
573 strived to measure and model MSW pyrolysis for a variety of configurations and operational
574 conditions. Although their findings well document the residence time as a function of drum
575 rotation frequency, surface roughness, etc., they found that there are significant distributions to
576 residence times, as well as significant differences when compared to normal distribution curves.
577 Fluidized-bed reactors offer higher heat transfer rates and better mixing, making them ideal for
578 fast pyrolysis [153]. Dai *et al.*[156], for example, studied the pyrolysis of waste tires in a
579 recirculating fluid bed. They found a multi-stage system was preferred for processing waste
580 materials like tires to ensure adequate residence time as well control the decomposition in several
581 stages to achieve high liquid yields. However, the application of fluid bed reactor in MSW is
582 limited by complications in separating materials and maintaining operational efficiency. Tubular
583 reactors present an innovative approach, allowing for continuous movement of material and
584 improved heat transfer. They generally involve a tubular housing, are externally heated, and use
585 mechanical transport of material down the length with a screw, scrapper, drag chain, etc. While
586 promising for future applications, they require rigorous pre-treatment of feedstock to avoid
587 operational challenges. Aguado *et al.* [157], for example, examined pyrolysis of low-density
588 polyethylene (LDPE) in a screw reactor. They found acceptable conversion of the hydrocarbon

589 chain over an acidic cracking catalyst resulted in acceptable selectivity (over 80%) to gasoline fuel
590 ranges, with overall increase in olefins with increasing transport speed with decreasing amounts
591 of paraffins, isoparaffins, and somewhat unchanging amount of naphthalenes, and aromatics.
592 Despite the promise of these pyrolysis technologies, they often face limitations. Pre-treatment
593 steps, such as separating contaminants and reducing moisture content, adding complexity and
594 increasing costs. Additionally, the need for effective emissions control is paramount, particularly
595 for harmful substances like HCl and SO₂ that can arise from certain feedstock components, such
596 as polyvinyl chloride (PVC). Emissions from these processes can include harmful gases such as
597 HCl, SO₂, and NH₃, which require careful management to minimize their impact on the
598 environment. Commercial pyrolysis systems often incorporate advanced scrubbing and filtering
599 techniques to address these emissions, positioning themselves as cleaner alternatives to traditional
600 incineration methods.

601 *2.2.4 Torrefaction*

602 Torrefaction, a thermochemical conversion process, operates under mild pyrolysis conditions
603 typically ranging from 200 to 350 °C in an oxygen-depleted environment [158-160]. The resultant
604 torrefied product, often termed "biocoal", exhibits characteristics akin to traditional coal, rendering
605 it suitable for co-firing with coal in power plants or direct utilization in industrial processes. The
606 benefits of torrefaction include an augmentation in fixed carbon content, calorific value, and
607 energy density [20, 21, 161, 162]. Furthermore, torrefaction enhances the grindability and
608 hydrophobicity of the solid products while reducing susceptibility to microbial degradation as
609 torrefaction reduces the moisture content significantly [2, 21, 163]. Critical process parameters
610 such as temperature, residence time, feedstock type, particle size, reactor type, moisture content,

611 and heating rate influence the physicochemical properties of torrefied material, with temperature
612 being the most influential, followed by residence time [164-166].

613 While torrefaction has traditionally been employed for upgrading biomass feedstocks, its
614 application to other feedstock types, such as MSW, sewage sludge is gaining attention. Research
615 have mainly been conducted to investigate the physical and chemical properties of torrefied MSW
616 [167-170]. Although literature on torrefaction technologies for MSW treatment is relatively scarce
617 compared to gasification and pyrolysis, it presents a promising avenue for addressing the
618 challenges associated with the direct utilization of MSW in thermochemical processes, such as
619 generates tar in gasification, produces water and acid contents in pyrolysis bio-oil, and releases
620 secondary pollutants during combustion [20]. Torrefaction showed the potential to solve the issues
621 associated with direct utilization of MSW. Studies have indicated that torrefaction can enhance the
622 physicochemical properties of MSW to levels comparable to coal [171]. Investigation into the
623 behavior of organic and inorganic pollutants during torrefaction reveals that heavy metals with
624 high boiling points (*e.g.*, Pb and Zn) tend to be retained in the char fraction, whereas those with
625 low boiling points, such as Hg, Cl tended to enter the gas phase [168, 172]. On the other hand,
626 organic pollutants such as dioxins are predominantly found in the char, with minor amounts in the
627 volatile fractions [172].

628 The primary objective of the study by Ivanovski et al. [171] was to investigate the effects of
629 torrefaction on the thermochemical properties of MSW sourced from the Republic of Slovenia.
630 The elemental composition of the raw MSW revealed a carbon content of 43.2%, hydrogen at
631 8.1%, nitrogen at 0.8%, oxygen at 47.9%, and sulfur at 0.03%. Proximate analysis indicated a
632 moisture content of 44.3%, volatile matter of 54.9%, fixed carbon content of 6.7%, and ash content
633 of 3.1%. The HHV of the raw MSW was determined to be 24.3 MJ/kg. The study found that

634 torrefaction significantly affects mass yield (MY) and energy yield (EY), with MY and EY
635 decreasing with increasing temperature: at 200°C, MY was 92.9% and EY 93.5%; at 250°C, MY
636 decreased to 79.1% and EY to 79.8%; and at 300°C, MY fell to 65.8% and EY to 66.8%. Compared
637 to traditional torrefaction literature, these trends in MY and EY are much different. While this
638 study with MSW shows a near 1:1 trend of decreasing MY to EY, for example, many biomass
639 torrefaction studies typically show more significant loss in MY with a relatively high retention in
640 EY closer to 2:1 or 3:1 ratio for decreasing MY to EY [21, 164, 173], significantly improving the
641 energy density. As a result, this suggests that while the properties of torrefied MSW chars may
642 perform better in combustion, the energy density is not significantly improved upon. Interestingly,
643 this seems to also be supported by investigations by Yuan *et al.* [167]. They note that although
644 torrefaction had a significant impact on the structure and size reduction properties of MSW, they
645 report very modest changes in ignition temperature, maximum weight loss, burnout temperature,
646 mean combustion rate, as well as combustible and burnout indices with torrefaction extent. Again,
647 biomass in comparison demonstrates more substantive changes in combustion properties with the
648 application of torrefaction [21].

649 The elemental analysis post-torrefaction of MSW showed an increase in carbon content to 52.9%
650 (at 300°C) and a decrease in hydrogen to 6.6%, while oxygen content declined to 39.5% [171].
651 The proximate analysis further revealed that fixed carbon increased to 10.1%, volatile matter
652 decreased to 44.7%, ash content rose to 6.6%, and HHV increased marginally to 25.3 MJ/kg. The
653 thermal analysis revealed distinct thermal stability zones for both raw and torrefied MSW samples.
654 The initial mass loss for raw MSW occurred around 74°C, corresponding to moisture evaporation,
655 followed by a significant degradation phase between 280°C and 360°C, where the weight loss was
656 notable, particularly for samples torrefied at 200°C and 250°C. In the higher temperature range, a

657 steady degradation phase was observed between 375°C and 615°C for all samples, culminating in
658 a final mass loss peak around 675-700°C, where the highest reaction intensity was recorded for
659 the 300°C torrefied chars, indicating enhanced stability and thermal degradation characteristics
660 with increasing torrefaction temperatures.

661 The study by Głód *et al.* [174] investigates the potential of torrefaction as a process to enhance the
662 energy properties of MSW, with more of a focus on the physical and mechanical properties of the
663 torrefied product. The findings demonstrate that torrefaction significantly improves the weather
664 resistance and durability of MSW pellets, allowing them to withstand prolonged immersion in
665 water without loss in structural integrity. Specifically, while untreated MSW pellets exhibited a
666 maximum water uptake of 0.72 kg of water/kg of fuel (dry) after 72 hours, torrefied pellets only
667 absorbed 0.34 kg of water/kg of fuel (dry), highlighting their enhanced hydrophobicity. These
668 water-resistant properties were also observed elsewhere [20]. Haykiri-Acma *et al.*[175], looked at
669 torrefaction following pelletization of a textile-rich RDF and found that all ranges of torrefaction
670 (230-290°C) improved water resistance time (maintaining pellet integrity) to >10 days, which was
671 the maximum testing time for that property. They also found that after 25 days the HHV for all
672 conditions changed less than 4%, with the most severe torrefaction case changing only 1%
673 indicating great potential for weather resistance and storage performance. Recent study by
674 Abdulyekeen *et al.* [20] demonstrated the efficacy of torrefaction in enhancing the hydrophobicity
675 and grindability of MSW. They reported that the torrefied MSW generates finer particles compared
676 to untreated samples, attributed to increased brittleness with torrefaction severity which agreed
677 with other literature [21, 176]. Measurement of contact angles confirms the improvement in
678 hydrophobicity, with torrefied MSW exhibiting significantly higher contact angles compared to
679 untreated MSW. For example, the contact angles measured for untreated and torrefied (at 300 °C

680 for 50 min) MSW were measured as 114.3° and 173.3°, respectively. Głód *et al.* [174] went on to
681 document that torrefaction leads to the production of stronger pellets with improved mechanical
682 properties, such as higher durability, compressive strength (3.75 MPa compared to 2 MPa), and
683 shear strength (34 MPa compared to 8 MPa), and as evidenced by values exceeding 99% durability
684 and compressive strengths greater than 3 MPa for all torrefied pellets. Another study looked at
685 extrusion, as another form of densification, of raw and torrefied combinations of waste plastics
686 and biomass [21]. They found that torrefaction of the waste mixtures generally improves the shear
687 strength of extruded filaments, but these properties were lower than those of virgin resins alone.
688 They suggest that, depending on the plastic type(s), the unmodified plastic exhibits an initial brief
689 elastic region followed by a prolonged strain hardening phase. When biomass fibers are added (or
690 other MSW fiber components, by analogue), the material behavior changes to a rapid brittle failure
691 with comparatively little strain. This suggests that the mixed pellets/filaments are much less
692 flexible, likely due to an influence of short fiber length and ineffective reinforcement from
693 interfacial shear stresses between the biomass and plastic regions. However, when pelletization is
694 used before torrefaction, it was found that torrefaction can decrease the strength as measured
695 through the compressive strength and hardness with increasing torrefaction[175]. For these
696 torrefied RDF pellets, a low torrefaction condition (230 °C) did not change the strength properties
697 from the raw RDF pellets drastically (1198 and 117 N/mm² for compressive strength and hardness
698 respectively, compared to 1141 and 112 N/mm²).

699 The milling of torrefied MSW also results in smaller average particle sizes and improved
700 grindability, as indicated by reduced Hardgrove Grindability Index (HGI) values (17 compared to
701 22 for HGI and 6 compared to 12 following Thermally Treated Biomass Grindability Index
702 (TTBGI) methods), suggesting a decrease in energy consumption during size reduction [174]. This

703 was also observed in simulated MSW streams and post-industrial wastes [20, 176]. Size reduction
 704 improvements were also observed for torrefaction of wood waste and garden wastes extracted from
 705 MSW streams [177]. Similar to the alteration of structural/strength properties discussed above, the
 706 authors attribute this to an embrittled structure and disrupted fibrous nature from partial
 707 degradation. In general, IR analysis of surface functional groups showed mostly loss of aliphatic
 708 and hydroxyl groups, while promoting increased aromatic groups. For example, increasing
 709 torrefaction severity showed less prominent bands (from dehydration reactions) at the 3500 and
 710 3750 cm^{-1} regions, represents the stretching vibration of hydroxyl (O–H) [178]. Table 2 and Table
 711 3 summarize the overall influences of torrefaction on waste feedstock size reduction and
 712 properties. These enhancements collectively indicate that torrefaction can effectively upgrade the
 713 physical and thermal characteristics of MSW, making it a more viable and efficient option for
 714 energy production.

715 *Table 2: Grindability characteristics of torrefied MSW and component fractions.*

Feedstock		Grindability Index (HGI/TTBGI)	Energy Consumption	Particle Size Distribution	Key Observations	Ref.
Biomass	Alder chips	HGI increased from ~20 to ~40	↓ by ~30–50% after torrefaction	Finer particles, narrower distribution	Significant improvement in grindability; suitable for vertical spindle mills	[179, 180]
	Willow chips	HGI increased from ~25 to ~45	↓ by ~40%	Improved uniformity	Excellent milling performance post-torrefaction	
	Palm kernel shells	HGI increased (exact values not given)	Not specified	Improved size reduction	High-density biomass showed better grindability after torrefaction	
	Biomass pellets (various)	Modified HGI used (varied by feedstock)	Cutting mill: 5.15 Wh/kg; Hammer mill: 5.24 Wh/kg; Impact mill: 8.23 Wh/kg	Cutting mill: 0.62 mm; Hammer mill: 0.51 mm; Impact mill: 0.41 mm	Impact mill produced finest particles; energy use varied by mill type	[181, 182]
MSW and Wastes	Mixed MSW (general)	TTBGI ↓ from 22 to 17	↓ (qualitative)	Smaller average particle size	Embrittlement improved grindability and reduced energy input	[20]
	Textile-rich RDF	TTBGI ↓ from 12 to 6	↓ (qualitative)	Maintained pellet integrity >10 days	Improved grindability and water resistance of RDF pellets	
	Wood/Garden waste	Not specified	↓ (qualitative)	Improved brittleness and size reduction	Fibrous structure disrupted, aiding mechanical processing	
	Paper/Cardboard	Not specified	↓ (qualitative)	Uniform particle size after pelleting	Pellets achieved >99% durability and >300 kg/m^3 density	[183]
	Thin plastics	Not suitable for pelleting	Not reported	Poor grindability	High moisture and elasticity hindered	

					densification and grinding	
Thick plastics	Not specified	Moisture ↓ by 30% (screw press)	Limited grindability improvement		Mechanical preprocessing improved dewatering but not grindability	
Paper-plastic blend	Similar to PRB coal (qualitative)	Not specified	Fiber → fine fraction; plastic → coarse		Torrefied blend showed coal-like grinding behavior; fiber and plastic separated by size	[176]
C&D waste	Not specified	3862–4338 MJ/t (torrefaction energy)	Improved grindability with power level ↑		Higher torrefaction power improved grindability and carbon content	[170]
Grass clippings	Not specified	↓ with higher moisture	Improved grindability at 64% m.c.		High moisture enhanced torrefaction efficiency and grindability	
MSW-derived pellets	Not specified	↓ by ~30–50%	Narrower particle size distribution		Torrefaction improved pellet brittleness and reduced milling energy	[20, 176]

716

717 The grindability of torrefied materials varies significantly between biomass and MSW
718 components, reflecting differences in composition, structure, and response to thermal treatment.
719 For biomass, torrefaction consistently improves grindability, as evidenced by substantial increases
720 in HGI. For example, alder and willow chips show increases from ~20–25 to ~40–45—and
721 reductions in energy consumption by 30–50%. These improvements are accompanied by finer and
722 more uniform particle size distributions, making torrefied biomass more suitable for pulverized
723 fuel systems. In contrast, MSW components exhibit more heterogeneous responses. Mixed MSW
724 and textile-rich RDF show notable improvements in grindability, with TTBTGI values decreasing
725 from 22 to 17 and 12 to 6, respectively, and enhanced brittleness facilitating size reduction. Paper
726 and cardboard fractions form durable, uniform pellets, while plastics, especially thin films, remain
727 challenging due to poor densification and elasticity. Blends of paper and plastic exhibit coal-like
728 grinding behavior, with fiber and plastic separating into fine and coarse fractions, respectively.
729 Other MSW-derived materials, such as construction and demolition waste or grass clippings, also
730 benefit from torrefaction, particularly under optimized moisture and power conditions. Overall,
731 while torrefaction enhances grindability across most MSW fractions, the degree of improvement
732 is highly dependent on feedstock type, preprocessing, and torrefaction severity.

733

Table 3: Torrefaction performance metrics by MSW component.

MSW Component	MY (%)	EY (%)	HHV Improvement (MJ/kg)	Hydrophobicity	Grindability	Ref.
Food waste	34–66	83–97	+5.9 (e.g., 11.1 → 17.0)	Improved (moisture resistance ↑)	Improved (due to embrittlement)	[184]
Plastics (LDPE, PET)	14–15	High (inert)	+5.3 (e.g., 19.2 → 24.5)	Low (hydrophobic by nature)	Low (no significant change)	[185]
Paper/Cardboard	~50–70	~60–80	+3–5	Moderate	Moderate	[20, 176]
Textiles (cotton/polyester)	40–60 (cotton-based)	50–70	+4–6 (lignite-equivalent)	Moderate	Improved (cotton-rich blends)	[186]
Yard waste	50–70	70–98	+6.6 (e.g., 15.6 → 22.2)	High (OH group loss)	High (fibrous structure breaks down)	[187]
Mixed MSW	51–70	65–85	+4–8 (e.g., 17.9 → 25.9)	Improved (O/C ↓)	Improved (ash and fiber breakdown)	[20]

734

735 Torrefaction performance varies significantly across different MSW components due to their
736 diverse physical and chemical compositions. MY typically decreases with increasing torrefaction
737 severity, with values ranging from 34–66% for food waste and up to 70% for yard waste and mixed
738 MSW. However, EY often remains relatively high (65–97%), particularly for food waste and yard
739 waste, due to the retention of energy-dense carbon fractions. HHV improvements are most
740 pronounced in lignocellulosic materials such as yard waste and paper/cardboard, where increases
741 of 4–6 MJ/kg are common, while plastics and textiles show more modest gains or inert behavior.
742 Hydrophobicity generally improves across all organic MSW types due to the loss of hydroxyl
743 groups and reduction in oxygen content, with torrefied food waste and yard waste exhibiting
744 enhanced moisture resistance. Grindability is also enhanced in fibrous or brittle materials like yard
745 waste and textiles, where torrefaction disrupts the structural integrity and facilitates size reduction.
746 In contrast, plastics such as LDPE and PET remain largely inert under typical torrefaction
747 conditions, showing minimal changes in grindability or hydrophobicity. These findings underscore
748 the importance of feedstock-specific strategies when applying torrefaction to MSW, particularly
749 when targeting downstream applications such as co-firing, pelletization, or gasification.

750 During torrefaction of comingled wastes, Rago *et al.*[188] documented synergistic interactions
751 between components. The study investigates the torrefaction of waste biomass, newspaper, and
752 low-density polyethylene, and their blends at 300°C. Notable synergistic interactions were
753 observed between the biomass and newspaper, leading to improved fuel properties in the resulting
754 char, such as increased HHV, higher carbon content, and reduced volatile matter content. These
755 interactions were statistically significant and resulted in enhanced devolatilization reactions, which
756 contributed to the improved fuel characteristics of the torrefied blend. In contrast, LDPE remained
757 largely inert at the torrefaction temperature, leading to inhibited mass transfer during co-
758 torrefaction with biomass. This resulted in higher char yield and HHV for biomass-LDPE blends,
759 but also in higher volatile matter content. They suggest that the plastic melt formed a coating
760 around biomass particles, which blocked the pores in the char matrix and limited the release of
761 volatiles, thereby promoting secondary char formation. Saha et al., also investigated synergistic
762 interactions of torrefied components in a study look at torrefaction (200-250°C) of mixed
763 biomasses (corn stover and loblolly pine) and various plastics (PET, HDPE, PVC, LDPE, PP, PS,
764 Polyurethane (PU), Nylon 6/6 (N66), Acrylonitrile butadiene styrene (ABS), and Polycarbonate
765 (PC)) [189]. Similar to the work of Rago, they also concluded that LDPE was effectively inert
766 during torrefaction and did not accelerate decomposition. However, they did not report that certain
767 plastics, namely PVC and PU, were most commonly associated with enhanced and degraded
768 reaction rates (synergy) respectively. In the case of negative synergy, they theorized that, similar
769 to Rago's conclusions [188], the degradation of PU formed a boundary layer (of char in this case)
770 around the fiber particles, reducing the overall volatile release rate. On the other hand, positive
771 synergy was noted to occur due to the formation of reactive intermediates that could catalyze
772 decomposition. HCl formation from dehydrochlorination, or formation of allylic radicals from

773 dehydrochlorination or hydrogen abstraction could enhance the breakdown of biomass through
774 attacking hydroxyl sites along the biopolymers. Similar effects were also noted by Zhu *et al.* [190]
775 in a kinetic study of mixed waste paper and plastics.

776 Torrefaction approaches for MSW present various advantages and limitations that influence their
777 effectiveness as a pretreatment method. Unfortunately, much existing literature knowledge is
778 based on biomass which has significantly different compositions, contaminations, physical
779 properties and formats [174]. Nevertheless, there are some technological advantages and shortfalls
780 that can be gained from existing work. Dry torrefaction significantly enhances the heating value
781 and energy density of biomass [191], while improving combustion stability and gasification quality
782 [192, 193]. However, it requires pre-drying of high-moisture feedstocks, which can be energy-
783 intensive, and may result in increased ash content, potentially leading to ash-related issues during
784 combustion [192, 194]. On the other hand, wet torrefaction eliminates the need for pre-drying,
785 thereby saving energy consumption and reducing ash content, which improves overall fuel
786 properties [195, 196]. Despite these benefits, wet torrefaction poses challenges such as equipment
787 corrosion, clogging, and the necessity for wastewater treatment and management, along with
788 producing a lower yield of torrefied product [193, 197]. Ionic-liquid-assisted torrefaction enhances
789 the rate and quality of biomass processing while utilizing environmentally friendly and recyclable
790 ionic liquids [198, 199], yet it is hindered by lower energy yields compared to dry torrefaction,
791 high operational costs, and limited commercial applicability. Super-heated steam torrefaction
792 minimizes carrier gas usage and enhances product uniformity, reducing explosion risks [200];
793 however, it necessitates specialized equipment for steam generation and control, which can be
794 costly and limit scalability. Lastly, microwave-assisted torrefaction improves energy yield,
795 grindability, and energy density of torrefied biomass with faster processing times and more

796 uniform product distribution [201]. Nevertheless, this method requires careful optimization of
797 microwave power and processing parameters, and it faces limitations in scalability due to the
798 complexity and costs of the necessary equipment.

799 From the above discussion, it can be summarized that although torrefaction is being widely used
800 as conversion pathway for biomass to produce high value fuels or products, for MSW it would be
801 better suited as a preprocessing step.

802 **2.3 Wet processes**

803 *2.3.1 Hydrothermal carbonization (HTC)*

804 Hydrothermal carbonization (HTC) is an emerging thermal conversion process that holds promise
805 for converting organic waste into an aqueous environment at elevated temperatures typically 180-
806 260°C and saturated pressures [202-206]. One of the main advantages of HTC is that it does not
807 require removing moisture from the feedstock to be processed. Unlike conventional torrefaction,
808 HTC is carried out in presence of subcritical water [207]. Under these conditions, organic
809 compounds undergo hydrolysis, dehydration, decarboxylation, and polymerization reactions.
810 These chemical transformations reduce the hydrogen and oxygen content in the feedstock while
811 concentrating carbon in the formation of a carbonaceous solid known as hydrochar, along with
812 aqueous by-products [208]. Batch experiments have shown that 45-75% of the carbon initially
813 present in the MSW feedstock is retained in the hydrochar [209]. The hydrochar produced exhibits
814 properties similar to lignite coal, with high carbon content and energy density [210]. If the
815 hydrochar is applied in scenarios involving long-term carbon storage, the overall greenhouse gas
816 emissions are typically lower than those associated with conventional waste management options
817 such as landfilling, composting, or incineration [211]. This makes HTC particularly attractive for
818 both energy recovery and carbon sequestration purposes.

819 Process conditions such as temperature and residence time play a critical role in determining the
820 yield and quality of the hydrochar. Increasing the severity of HTC (*i.e.*, higher temperatures or
821 longer reaction times) typically reduces solid yields but increases the fixed carbon content, HHV,
822 and degree of carbonization. Lucian *et al.* [212] demonstrated that under intermediate HTC
823 conditions 220-240 °C, secondary chars can condense on the surface of primary hydrochar. These
824 secondary chars, extractable with organic solvents, are rich in compounds such as phenols,
825 furfurals, and organic acids. They may enhance the reactivity and energy content of the final
826 product but also present potential challenges for product purity and downstream processing.

827 In support of these observations, a comparison of key literature values related to hydrochar
828 properties under different HTC conditions is presented in Table 4. The table includes data on
829 elemental composition C, H, N, S, O wt%, proximate analysis including volatile matter, fixed
830 carbon, ash wt%, and HHV, as functions of process temperature and duration. Notably, increasing
831 the HTC temperature results in higher carbon content and HHV while reducing oxygen content.
832 For instance, at 230 °C for 45 minutes, the hydrochar in Abdoli *et al.* [213] reached 66.6 wt% C
833 and an HHV of 27.64 MJ/kg, compared to only 43.5 wt% C and 19.5 MJ/kg at 180 °C for 60
834 minutes reported by Lucian *et al.* [214]. This aligns with the chemical transformations that remove
835 oxygen-containing functional groups and enhance energy density. Additionally, fixed carbon
836 increases with severity, from 35.1 wt% at 180 °C to 49.2 wt% at 260 °C, while volatile matter
837 decreases, indicating improved combustion behavior. Ash content remains relatively stable across
838 conditions 6-9 wt%, though feedstock variability may influence this. Nitrogen and sulfur contents
839 were low across all studies reported here, although it will change with feedstock type. These
840 studies typically showed decreasing S and increasing N with more intense processing.

841 HTC has also demonstrated versatility in handling the heterogenous and variable nature of MSW.
842 Researchers have investigated the carbonization of individual MSW components such as food
843 waste, paper, wood, rubber, and plastics to better understand how each behaves under
844 hydrothermal conditions. Lin *et al.* [215] found that HTC significantly improves fuel properties
845 and thermal stability of lignocellulosic components such as paper and wood. However, food waste
846 undergoes extensive solubilization and decomposition, which diminishes the combustion
847 improvement of the resulting hydrochar. Additionally, polymers such as PP and PE undergo
848 minimal chemical transformation during HTC, indicating that HTC is better suited to biogenic
849 fractions of MSW [216].

850 Environmental assessments have shown that HTC may provide sustainable performance compared
851 to other waste management strategies. A recent LCA study by Mannarino *et al.* [217] evaluated
852 the integration of HTC into a water resource recovery facility treating sewage sludge. The study
853 compared four HTC-based scenarios with a benchmark composting strategy and found that HTC
854 could reduce climate change impacts by up to 98% relative to composting. Moreover, when the
855 process water from HTC was subjected to anaerobic digestion (AD) for biogas recovery,
856 environmental performance improved across 11 of 16 impact categories. Furthermore, when
857 hydrochar is combusted for energy recovery, the net calorific value often exceeds that of biogas
858 generated via AD or the direct incineration of raw MSW [213]. Moreover, HTC produces fewer
859 emissions than incineration and offers solid fuel that is more hydrophobic, dense, and stable,
860 improving its storage, handling, and transport properties [209, 215].

861 An increasingly popular direction involves the integration of HTC with AD, a biological process
862 where microorganisms break down organic matter in the absence of oxygen. In such hybrid
863 systems, the digestate produced from AD can undergo HTC to generate additional hydrochar,

864 while the process water from HTC can still retain biodegradable compounds that support further
865 methane production [218]. In typical AD-only configurations for treatment of MSW, 305-3850
866 mg/L of the influent chemical oxygen demand (COD) remains in the digestate, whereas HTC of
867 this digestate can recover 64-88% of its dry mass as hydrochar and transfer 9.58-72.3 g/L of soluble
868 organics into the process water, when this HTC liquid or slurry is recycled to AD, Aragón-Briceño
869 et al. [219] and others report biomethane increases of up to 80% in HTC process water, compared
870 with untreated organic fraction substrates [220, 221]. This coupling enhances recourse recovery
871 and promotes a more circular treatment pathway. For example, *Lucian et al.* [214] and Sharma et
872 al. [222] reported that HTC of the organic fraction solid digestate produced after AD of the organic
873 fraction of municipal solid waste, containing a stabilized but still organic-rich fraction along an
874 inorganic/ash fraction not only improved hydrochar quality but also yielded process water suitable
875 for subsequent AD, by partially depolymerizing residual solids, increasing soluble COD and
876 volatile fatty acids, and generating an aqueous phase that remained biodegradable even though the
877 parent solids had already undergone AD, enabling multiple valorization routes within the same
878 waste stream [222]. In this context, HTC acts as a post-treatment that disrupts lignocellulosic and
879 microbial structures left in the digestate, converting hard-to-digest solids into more enzyme
880 accessible substrates for a second AD step rather than simply retreating fully stabilized material.

881

Table 4: Characteristics of MSW derived hydrochar at different conditions. NR indicates “not reported” in the literature.

HTC condition		Ultimate analysis, db (%)					Proximate analysis, db (%)			HHV, db (MJ/kg)	Ref.
Temp. (°C)	Time (min)	C	H	N	S	O	VM	FC	Ash		
200	30	49.19	6.36	2.06	0.33	42.06	88.21	10.18	1.61	NR	[48]
200	30	35.5 ± 8.1	4.57 ± 0.7	1.5 ± 0.3	<0.1	34.6 ± 1.8	62.5 ± 1.1	11.1 ± 2.5	26.4 ± 1.4	17.4 ± 0.6	[223]
200	120	45.4 ± 9.8	5.01 ± 0.2	1.5 ± 0.4	<0.1	35.1 ± 0.7	65.0 ± 0.9	10.9 ± 1.7	24.1 ± 0.8	16.8 ± 0.5	
250	30	39.9 ± 4.7	4.76 ± 0.3	1.9 ± 0.3	<0.1	25.5 ± 1.4	47.0 ± 0.8	16.4 ± 3.4	36.6 ± 2.6	18.0 ± 0.8	
250	120	42.6 ± 2.2	4.38 ± 0.0	2.2 ± 0.1	<0.1	19.0 ± 1.0	43.4 ± 1.0	17.5 ± 2.6	39.1 ± 1.6	18.9 ± 2.7	
300	30	42.5 ± 5.6	4.54 ± 0.2	2.3 ± 0.3	<0.1	15.7 ± 1.6	41.3 ± 3.9	15.6 ± 4.0	46.1 ± 5.1	20.7 ± 1.7	
300	120	43.9 ± 0.1	4.00 ± 0.1	2.3 ± 0.0	<0.1	15.7 ± 0.6	40.2 ± 1.5	20.3 ± 4.9	39.5 ± 3.4	21.0 ± 0.6	
190	30	56.85	7.33	0.97	0.08	32.59	75.16	23.76	1.09	19.05	[224]
250	1200	33.5	2.7	0.63	0.05	14.2	35.7	5.5	48.8	20.0	[225]
NR	NR	23.63	1.07	2.60	NR	35.04	52.99	9.35	37.66	NR	[225]
NR	NR	47.36	8.56	1.78	0.38	23.01	69.71	11.38	18.91	NR	[226]
150	30	60.87	8.35	0.79	0.11	29.88	80.77	13.24	5.99	30.17	[227]
175	30	63.81	8.81	0.72	0.11	26.55	79.27	14.58	6.15	30.77	
200	30	66.55	8.78	0.70	0.10	23.87	76.16	18.39	5.45	33.01	
225	30	70.54	8.97	0.60	0.08	19.81	78.75	15.92	5.33	36.69	
210	30	33.89	4.63	1.42	1.09	15.12	43.3 ± 0.5	12.8 ± 0.5	43.9 ± 0.7	13.5 ± 0.1	[228]
230	30	34.39	4.76	1.04	0.74	13.98	41.5 ± 0.7	13.4 ± 0.8	45.1 ± 0.5	14.2 ± 0.0	
250	30	35.04	4.57	1.41	0.67	5.37	34.4 ± 0.4	12.6 ± 0.9	53.0 ± 0.6	14.6 ± 0.1	
280	30	35.58	4.19	1.54	0.43	3.34	33.0 ± 0.8	12.1 ± 1.4	54.9 ± 0.9	15.2 ± 0.0	
210	60	33.61	4.24	1.13	0.92	14.16	41.5 ± 0.3	12.5 ± 0.3	45.9 ± 0.4	13.7 ± 0.0	
230	60	34.81	4.74	1.09	0.57	9.57	38.1 ± 0.2	12.7 ± 0.3	49.2 ± 0.3	14.3 ± 0.0	
250	60	34.71	3.45	1.31	0.54	6.09	34.3 ± 0.2	11.8 ± 0.6	53.9 ± 0.7	14.7 ± 0.1	
280	60	35.69	3.33	1.54	0.43	4.36	33.2 ± 0.9	12.2 ± 1.0	54.7 ± 0.5	15.4 ± 0.1	
210	90	33.15	4.26	0.86	0.83	12.14	39.7 ± 0.3	11.6 ± 0.4	48.8 ± 0.6	14.1 ± 0.1	
230	90	36.58	4.32	1.34	0.52	6.39	36.9 ± 0.3	12.2 ± 1.0	50.9 ± 0.7	14.3 ± 0.1	
250	90	30.45	3.30	1.38	0.5	4.00	29.9 ± 0.2	9.7 ± 1.0	60.4 ± 0.8	14.6 ± 0.1	
280	90	28.90	3.28	1.42	0.33	3.96	28.6 ± 0.4	9.3 ± 0.8	62.1 ± 1.2	14.8 ± 0.1	
180	60	43.3	5.4	1.4	NR	33.3	82.2	1.1	16.7	19.5	[229]
180	180	44.4	5.4	2.0	NR	29.0	78.3	2.4	19.3	18.9	
220	180	53.5	5.9	2.0	NR	20.8	71.1	11.1	17.8	22.2	
250	360	57.3	5.6	2.7	NR	6.2	55.0	16.8	28.2	25.6	

884 An emerging and underexplored opportunity is the use of HTC as a pretreatment step for high-
885 temperature thermochemical conversions such as pyrolysis, gasification, or combustion. While
886 direct studies on MSW are limited, there is compelling evidence from biomass-focused research
887 that HTC-treated solids possess favorable structural and chemical characteristics that enhance
888 performance in downstream thermal processes. Specifically, studies from, Islam *et al.* [230] and
889 Fakudze *et al.* [231], demonstrate that HTC produces char with improved thermal stability,
890 reduced reactivity to moisture, and higher aromaticity. These traits translate to better handling,
891 reduced tar formation in gasifiers, and improved calorific content in combustion [232].
892 Furthermore, HTC offers partial demineralization and homogenization of heterogeneous
893 feedstock, including waste and mixed biomasses, and MSW, facilitating smoother operation and
894 longer lifespans for reactors used in pyrolysis or combustion [225]. Integrating HTC upstream of
895 these high-temperature processes could represent a viable pathway to improve both operational
896 efficiency and product quality but experimental data specifically applying this strategy to MSW
897 remains a critical research gap.

898 Despite its promise, HTC is not without challenges. One major concern is the fate of inorganic
899 components, such as chlorine, sodium, and potassium, which may remain in the hydrochar or leach
900 into the process water. These inorganics can negatively affect the combustion characteristics or
901 require additional downstream treatment to mitigate environmental risks. Furthermore, the
902 aqueous phase contains a variety of dissolved organic compounds some of which may be inhibitory
903 or difficult to degrade which complicates its treatment and potential reuse [233]. When processing
904 MSW, there are components such as plastics rubber, synthetic textiles, etc. that are not
905 significantly degraded [216]. As a result, the applications of MSW solid chars may need to be used
906 differently than biomass derived chars. Lastly, scalability and economic viability of HTC remain

907 uncertain. Limited commercial-scale deployment exists, and questions remain regarding the cost
908 of reactor materials, heat recovery, process integration, and the market for hydrochar products.

909 2.3.2 *Hydrothermal liquefaction (HTL)*

910 Hydrothermal liquefaction (HTL) process can convert biomass, including the organic fraction of
911 MSW, into a crude-like bio-oil under subcritical water conditions, typically 260-375 °C and 10-
912 25 MPa [234-236]. Unlike pyrolysis and gasification, HTL operates in an aqueous medium,
913 making it especially suitable for wet feedstock without requiring energy-intensive drying. The
914 main products are biocrude oil, an aqueous phase rich in organic compounds, gaseous byproducts
915 (mainly CO₂), and solid char and ash residues [237].

916 HTL mimics natural petroleum formation on a vastly accelerated timescale by depolymerizing and
917 solubilizing organic polymers such as cellulose, hemicellulose, proteins, and lipids. The process
918 involves a series of reactions including hydrolysis, dehydration, decarboxylation, and cleavage of
919 carbon-nitrogen bonds [238]. When applied to MSW, HTL effectively reduces its volume and
920 converts its energy-rich organic fractions (*e.g.*, organic fraction, plastic) into a transportable and
921 upgradable biocrude. Importantly, HTL is tolerant of feedstock variability, accommodating a mix
922 of food waste, paper, yard waste, and biosolids, though optimal performance depends on proper
923 control of operating parameters such as temperature, residence time, and pH [239].

924 Macromolecular components of MSW, such as cellulose, hemicellulose, lignin, proteins, and lipids
925 undergo distinct transformation pathways [234, 235, 240]. Carbohydrates primarily hydrolyze into
926 sugars and subsequently dehydrate into furans and organic acids, while lignin decomposes into
927 phenolic compounds through cleavage of ether and carbon-carbon linkages. Proteins contribute to
928 nitrogen-containing intermediates, including amines and heterocyclic compounds, which can later

929 be incorporated into the biocrude. Lipids, when present, typically yield long-chain hydrocarbons
930 via hydrolysis and decarboxylation, contributing positively to fuel quality.

931 Secondary reactions play a critical role in determining product distribution. These include
932 polymerization and condensation reactions that convert reactive intermediates into heavier oil
933 fractions or solid char [241]. The balance between depolymerization and repolymerization
934 reactions is strongly influenced by temperature, residence time, and the presence of catalysts or
935 co-solvents [236]. Higher temperatures generally favor depolymerization and oil formation, while
936 excessive severity can promote gasification and char formation [237].

937 Several studies have explored the performance of HTL on MSW, examining not only yield but
938 also the quality of the resulting biocrude and the properties of the residual phases. For instance,
939 HTL applied to the organic fraction of MSW digestate, comprising primarily of anaerobically
940 digested food waste and sewage sludge, resulted in the production of a biocrude with enhanced
941 energy density (up to 34 MJ/kg), significantly reduced moisture content, and moderate heteroatom
942 levels [242]. Elemental analysis of the biocrude revealed carbon, hydrogen, nitrogen, and oxygen
943 contents of approximately 68.2%, 9.2%, 5.8%, and 15.3%, respectively, with sulfur content being
944 negligible [243]. These heteroatoms, particularly nitrogen and oxygen, are known to originate from
945 proteinaceous and carbohydrate-rich components of the feedstock and pose challenges for
946 downstream upgrading due to their impact on stability and emissions [242]. Pre-treatment methods
947 such as de-ashing and aqueous phase recirculation have also been found to influence biocrude
948 properties, with improvements in oil stability and reduction in inorganic contaminants [244].

949 Table 5 summarizes key data from selected studies on HTL of MSW, comparing temperature,
950 time, elemental composition, heating value, and yields. These results provide insight into how
951 process conditions affect the quality and energy density of HTL products. As shown in the HTL

952 literature comparison in Table 5, there is no consistent correlation between temperature, residence
953 time, and the HHV of biocrude when DI water is used as the sole solvent. For MSW feedstocks
954 processed in DI water, biocrude HHVs span a broad range (25.2–37.0 MJ/kg) across temperatures
955 of 200–360 °C and residence times of 20–60 minutes. These variations appear to be more strongly
956 influenced by differences in feedstock composition and product distribution than by a direct
957 dependence on temperature or time. In contrast, experiments employing a 1:1 DI water:glycerol
958 co-solvent system exhibit a more discernible relationship between temperature and biocrude
959 quality. At 300 °C, HHV remain relatively stable (28.5–30.7 MJ/kg) across residence times of 15-
960 45 minutes. However, increasing the temperature to 325–350 °C results in higher HHV (33.3–35.6
961 MJ/kg), accompanied by increased carbon content and reduced oxygen content in the biocrude.
962 These findings suggest that, within the co-solvent system, temperature exerts a more pronounced
963 and positive influence on biocrude energy content than residence time. The high HHVs in these
964 studies confirm that HTL biocrude is energetically competitive precursor compared to other
965 pathways. Across all studies, the nitrogen content remained moderately high 3-5 wt%, reflective
966 of the proteinaceous nature of food and green waste within MSW. Sulfur content was generally
967 low <0.6 wt%, reducing the risk of SO_x emissions upon combustion.

968 Recent studies have increasingly focused on HTL of real MSW feedstocks, enabling more realistic
969 evaluation of process performance, product quality, and operational challenges. These
970 investigations demonstrate that feedstock heterogeneity significantly influences reaction
971 pathways, biocrude yield, and composition, particularly due to the presence of mixed organic
972 fractions and inorganic contaminants such as alkali metals and chlorine. For instance, recent
973 studies on real MSW have shown that inorganic species can affect phase partitioning, promote side
974 reactions, and contribute to catalyst deactivation and increased heteroatom content in biocrude,

975 thereby complicating downstream upgrading processes [245, 246]. In addition, these studies report
976 that HTL of real MSW generates more complex aqueous and oil phases containing higher
977 concentrations of oxygenated and nitrogen-containing compounds, which further challenges
978 product stabilization and refining [244]. Overall, these recent advancements highlight that while
979 HTL offers strong potential for valorizing wet and heterogeneous MSW streams, effective
980 implementation requires improved understanding of feedstock variability, inorganic behavior, and
981 integrated upgrading strategies under realistic operating conditions. Successful implementation at-
982 scale will require holistic consideration of the inorganic fraction of its influence on oil quality,
983 wastewater burden, and solid residue utilization. Continued research into feedstock preprocessing,
984 catalytic stabilization, and circular economy integration will be essential to unlock the full
985 potential of HTL in sustainable waste management systems.

986 The presence of heteroatoms, particularly nitrogen and oxygen, poses challenges for downstream
987 upgrading. Nitrogen compounds can lead to NO_x emissions during combustion and catalyst
988 poisoning during hydrotreating, while oxygenated species reduce thermal stability and increase
989 acidity. As a result, upgrading processes such as hydrodeoxygenation and hydrodenitrogenation
990 are typically required to produce transportation-grade fuels [237, 242]. In addition, the aqueous
991 phase generated during HTL contains a significant fraction of dissolved organic compounds,
992 including short-chain acids, alcohols, phenols, and nitrogenous species. This phase often exhibits
993 high COD, which can complicate wastewater treatment but also presents opportunities for energy
994 recovery via AD or nutrient recovery [244, 247].

995 A critical challenge in HTL of MSW lies in managing the inorganic fraction of the feedstock.
996 MSW typically contains non-biodegradable components such as glass, metals, ceramics, and
997 mineral impurities, which are not reactive under HTL conditions and accumulate in the residual

998 solid phase or migrate into aqueous and oil fractions. Common inorganics such as sodium,
999 potassium, calcium, chlorine, phosphorus, and trace metals (*e.g.*, zinc, copper, iron) can
1000 significantly affect both process performance and downstream upgrading [248]. In the biocrude,
1001 alkali and alkaline earth metals (AAEMs) may promote emulsification, cause corrosion in
1002 upgrading reactors, and poison catalysts during hydrotreating. Their presence often necessitates
1003 additional demineralization steps such as solvent washing, adsorption, or ion exchange prior to
1004 catalytic upgrading [249]. In some cases, the solid residue can be processed into biochar or ash
1005 suitable for use as soil amendments or construction materials, particularly if heavy metal
1006 concentrations remain within regulatory limits [250]. Meanwhile, inorganics that partition into the
1007 aqueous phase can increase COD and toxicity, complicating wastewater treatment and limiting
1008 opportunities for reuse or nutrient recovery [247]. In some cases, the inorganic phosphorus in the
1009 aqueous phase could be recovered as struvite or phosphates, integrating HTL into nutrient recovery
1010 systems [251], however, these applications require careful leachate testing and compliance with
1011 environmental standards. Several mitigation strategies have been explored. Mechanical pre-sorting
1012 and size reduction can remove large non-reactive particles, while chemical pre-treatment such as
1013 acid washing can reduce ash-forming minerals before liquefaction. Additionally, recirculation of
1014 the aqueous phase has been shown to reduce the overall process water requirements, though care
1015 must be taken to avoid the buildup of inhibitory compounds or salinity [252]. Treatment strategies
1016 include biological processes (*e.g.*, AD), advanced oxidation, and membrane separation. In some
1017 cases, nutrient recovery, particularly phosphorus as struvite, can enhance the overall sustainability
1018 of the process.

1019 Although recent research has focused on improving HTL performance through catalytic systems
1020 and co-solvents, the integration of HTL with other thermochemical and biological processes

1021 represents a promising pathway for maximizing resource recovery. For example, coupling HTL
1022 with AD allows for the valorization of both solid and aqueous fractions, improving overall energy
1023 recovery [218, 222]. Similarly, integrating HTL upstream of gasification or catalytic upgrading
1024 can enhance feedstock uniformity and reduce tar formation[84].

1025

Table 5: Characteristics of MSW at different conditions. NR indicates “not reported” in the literature while b.d. represents “below detection limit”.

Reactants			HTL condition		HHV, db (MJ/kg)	Bio-oil ultimate analysis, db (%)					Mass yield, db (%)			Ref.
Feedstock	Solvent	Catalyst	Temp. (°C)	Time (min)		C	H	N	S	O	Solid	Oil	Gas	
Real-MSW	DI water	No	320	20	37.00	77.67 ± 0.68	8.90 ± 0.14	1.50 ± 0.10	NR	10.18 ± 0.22	12.9	26.8	14.1	[253]
Real-MSW	DI water	No	350	15	30.15	62.82	9.39	2.94	NR	24.86	54.17	10.57	NR	[245]
Real-MSW	DI water	Yes	350	15	28.61	60.28	9.20	3.36	NR	27.17	37.80	17.62	NR	
Real-MSW	DI water	No	200	60	33.5	57.40	12.80	4.90	0.50	24.40	NR	NR	NR	[239]
Biogenic-MSW	DI water	No	320	60	26.09 ± 1.65	62.50 ± 3.56	6.44 ± 0.65	7.31 ± 1.11	0.02 ± 0.02	23.73 ± 2.82	NR	NR	NR	[246]
Real-MSW	DI water	No	340	60	27.00 ± 1.72	64.90 ± 4.02	6.24 ± 0.90	7.27 ± 1.62	0.04 ± 0.02	21.55 ± 2.53	20.6	18.0	20.9	
Real-MSW	DI water	No	360	60	25.24 ± 1.59	63.50 ± 4.12	5.55 ± 0.72	7.67 ± 1.53	0.05 ± 0.01	23.23 ± 3.12	NR	NR	NR	
Real-MSW	DI water	No	300	30	NR	NR	NR	NR	NR	NR	90.4	6.0	3.6	[254]
Real-MSW	DI water	No	320	30	NR	NR	NR	NR	NR	NR	87.7	8.2	4.1	
Real-MSW	DI water	No	330	30	NR	NR	NR	NR	NR	NR	87.5	8.7	3.8	
Real-MSW	DI water	No	350	30	31.0	74.0	8.3	1.9	b.d.	14.8	81.4	15.2	3.4	
Real-MSW	1:1 DI water:Glycerol	No	300	15	30.7	67.4	7.6	0.6	b.d.	24.4	72.2	24.5	3.3	
Real-MSW	1:1 DI water:Glycerol	No	300	30	28.5	61.1	8.1	0.3	b.d.	30.5	68.5	26.2	5.3	
Real-MSW	1:1 DI water:Glycerol	No	300	45	28.7	62.3	7.8	0.4	b.d.	29.5	64.8	31.1	4.1	
Real-MSW	1:1 DI water:Glycerol	No	325	15	33.3	71.0	7.4	0.6	b.d.	21.0	46.2	48.1	5.7	
Real-MSW	1:1 DI water:Glycerol	No	325	30	33.5	73.0	7.6	0.8	b.d.	18.6	42.1	53.2	4.7	
Real-MSW	1:1 DI water:Glycerol	No	325	45	33.4	73.2	6.8	0.7	b.d.	19.3	40.4	55.8	3.8	
Real-MSW	1:1 DI water:Glycerol	No	350	15	33.4	74.2	7.7	0.8	b.d.	17.3	33.6	59.3	7.1	
Real-MSW	1:1 DI water:Glycerol	No	350	30	35.6	77.0	6.8	0.9	0.2	15.1	33.3	60.2	6.5	
Real-MSW	1:1 DI water:Glycerol	No	350	45	34.6	77.0	7.3	0.4	b.d.	15.3	32.1	61.6	6.3	

1028 **3 Conclusions and future recommendations**

1029 This review highlights the potential of thermochemical conversion processes as innovative
1030 solutions for managing MSW while simultaneously generating energy and value-added products.

1031 The advantages of these technologies over traditional incineration methods include enhanced
1032 energy efficiency, the production of high-quality fuels, and the integration of sophisticated
1033 pollution control measures. However, the inherent variability in MSW composition presents
1034 substantial challenges in optimizing these conversion processes. The variability in MSW
1035 composition, influenced by factors such as population density, economic activity, and seasonal
1036 fluctuations, necessitates comprehensive characterization efforts across diverse geographical
1037 regions. Future research should prioritize the development of standardized protocols for the
1038 systematic evaluation of MSW feedstocks to facilitate the optimization of thermochemical
1039 conversion technologies.

1040 Table 6 exhibits distinct trade-offs of thermochemical conversion technologies in terms of
1041 efficiency, scalability, product quality, and environmental performance. Combustion remains the
1042 most mature and scalable technology but is limited to energy recovery. In contrast, gasification
1043 and pyrolysis offer greater flexibility in producing fuels and chemicals, though they require more
1044 stringent feedstock control and downstream processing. Hydrothermal processes, particularly
1045 HTL, demonstrate strong potential for wet MSW streams by eliminating drying requirements and
1046 producing energy-dense fuels, but challenges related to inorganics, upgrading, and process
1047 integration still remain. Overall, no single technology is universally optimal; instead, hybrid
1048 systems that combine preprocessing (e.g., HTC or torrefaction) with high-temperature conversion
1049 pathways may offer the most effective route for maximizing resource recovery from MSW.

1050

Table 6: Comparative assessment of thermochemical conversion technologies for MSW.

Technology	Scalability	Feedstock flexibility	Product quality	Environmental impact	Key challenges	Overall assessment
Combustion	Commercial, large-scale	Very high (handles mixed MSW)	Low (no chemical products)	High emissions (NOx, dioxins) but controlled in modern systems	Low efficiency for material recovery, public perception	Mature, reliable but limited to energy recovery
Gasification	Demonstration –commercial	Moderate (requires preprocessing)	High (flexible fuel/chemicals)	Lower emissions than combustion; tar issues	Tar formation, feedstock variability, gas cleanup cost	Promising for chemicals and hydrogen production
Pyrolysis	Pilot–demonstration	Moderate (needs sorting/drying)	Variable (bio-oil instability)	Lower emissions; requires upgrading	Oil quality, heterogeneity, scale-up challenges	Flexible but still developing for MSW
Torrefaction	Pilot scale	Moderate	Moderate (improved fuel properties)	Low emissions	Limited energy densification for MSW	Best as preprocessing step
HTC	Emerging	High (wet feedstocks)	Moderate (solid fuel)	Lower emissions, potential carbon sequestration	Wastewater treatment, limited plastic conversion	Strong for wet MSW pretreatment
HTL	Pilot–early commercial	High (wet, mixed organics)	High (energy-dense oil)	Lower air emissions; wastewater concerns	Heteroatoms, upgrading, inorganics, cost	Highly promising for fuel production from wet MSW

1051

1052 An integrated waste management system incorporating various pretreatments is often necessary,
1053 including mechanical, biological, and heat treatments. The objective of such preprocessing is to
1054 enhance waste combustibility and maximize the recovery of recyclable materials. In addition to
1055 these pretreatment methods, torrefaction can also be employed to reduce moisture content and
1056 produce MSW-derived fuel for subsequent thermochemical conversion. This integration of low
1057 temperature technologies such as HTC and HTL with traditional thermochemical conversion
1058 methods presents a promising avenue for improving feedstock quality. Future work should focus
1059 on specific hybrid system configurations, such as: (i) HTC coupled with gasification to improve
1060 feedstock uniformity and reduce tar formation, (ii) HTL integrated with catalytic upgrading or
1061 refinery co-processing to produce transportation-grade fuels, (iii) HTL combined with AD to
1062 valorize aqueous byproducts and enhance overall energy recovery, and (iv) pyrolysis systems
1063 coupled with catalytic reforming to improve bio-oil stability and quality. These targeted
1064 configurations provide a clearer pathway toward scalable and efficient MSW valorization systems.
1065 Future studies should also explore the synergistic effects of these integrated approaches, with a
1066 focus on optimizing operating parameters to maximize efficiency and reduce pollutant formation.

1067 Investigating these pathways will require experimental validation using real MSW feedstocks
1068 instead of synthetic and/or part of MSW, alongside techno-economic assessments to evaluate their
1069 feasibility and scalability.

1070 While parametric and exploratory investigations of reaction conditions and various technologies
1071 are essential, there is an apparent gap in current literature that looks holistically at the impacts such
1072 systems could have. As much care should be taken into characterization, remediation, and
1073 demonstration of safe waste disposal, greater attention must be given to key unresolved
1074 challenges, including: (i) the behavior and partitioning of inorganic species such as alkali metals,
1075 chlorine, and heavy metals and their impacts on corrosion, fouling, and catalyst deactivation; (ii)
1076 the upgrading of intermediate products such as bio-oil and biocrude, particularly with respect to
1077 heteroatom removal and fuel stability; and (iii) the treatment and valorization of aqueous
1078 byproducts from HTL and HTC, including opportunities for COD reduction, nutrient recovery,
1079 and integration with biological systems such as AD.

1080 Further, the challenges associated with emissions control, particularly with respect to harmful
1081 pollutants generated during conversion processes, cannot be overlooked. Investment in advanced
1082 emission control technologies and the implementation of rigorous monitoring protocols will be
1083 critical to ensure compliance with environmental regulations and to build public trust in WtE
1084 facilities. In parallel, there is a growing need for integrated techno-economic and life-cycle
1085 assessment studies that evaluate entire systems rather than individual processes, incorporating
1086 feedstock variability and regional waste management conditions. Additionally, the application of
1087 digital tools such as machine learning and advanced process modeling offers promising
1088 opportunities for improving process control, optimizing operating conditions, and enhancing
1089 system reliability.

1090 In conclusion, while the thermochemical conversion of MSW shows great promise for sustainable
1091 waste management and energy recovery, continued research must move beyond isolated process
1092 evaluation toward integrated, scalable, and system-level solutions. Collaborative efforts among
1093 researchers, policymakers, and industry stakeholders will be critical to promote innovation and
1094 facilitate the broader adoption of effective WtE strategies.

1095 **Acknowledgement**

1096 The research is supported by the U.S. Department of Energy (DOE), Office of Energy Efficiency
1097 and Renewable Energy (EERE), Bioenergy Technologies Office (BETO), under DOE Idaho
1098 Operations Office with Contract No. DE-AC07-05ID14517.

1099

1100

1101 References

- 1102 [1] U.S.E.P. Agency, National Overview: Facts and Figures on Materials, Wastes and Recycling,
1103 in, 2018.
- 1104 [2] L. Matsakas, Q. Gao, S. Jansson, U. Rova, P. Christakopoulos, Green conversion of municipal
1105 solid wastes into fuels and chemicals, *Electronic Journal of Biotechnology*, 26 (2017) 69–83.
- 1106 [3] N. Saha, J. Klinger, M.T. Islam, T. Reza, Advanced biorefinery feedstock from non-recyclable
1107 municipal solid waste by mechanical preprocessing, *Frontiers in Fuels*, 1 (2023) 1105637.
- 1108 [4] T. Karak, R. Bhagat, P. Bhattacharyya, Municipal solid waste generation, composition, and
1109 management: the world scenario, *Critical reviews in environmental science and technology*, 42
1110 (2012) 1509–1630.
- 1111 [5] D.M.-C. Chen, B.L. Bodirsky, T. Krueger, A. Mishra, A. Popp, The world’s growing municipal
1112 solid waste: trends and impacts, *Environmental Research Letters*, 15 (2020) 074021.
- 1113 [6] I. Pecorini, E. Rossi, R. Iannelli, Bromatological, proximate and ultimate analysis of OFMSW
1114 for different seasons and collection systems, *Sustainability*, 12 (2020) 2639.
- 1115 [7] Y. Du, T. Ju, Y. Meng, T. Lan, S. Han, J. Jiang, A review on municipal solid waste pyrolysis
1116 of different composition for gas production, *Fuel processing technology*, 224 (2021) 107026.
- 1117 [8] M. Horttanainen, N. Teirasvuori, V. Kapustina, M. Hupponen, M. Luoranen, The composition,
1118 heating value and renewable share of the energy content of mixed municipal solid waste in Finland,
1119 *Waste management*, 33 (2013) 2680–2686.
- 1120 [9] Z.u. Rahman, X. Wang, J. Zhang, Z. Yang, G. Dai, P. Verma, H. Mikulcic, M. Vujanovic, H.
1121 Tan, R.L. Axelbaum, Nitrogen evolution, NOX formation and reduction in pressurized oxy coal
1122 combustion, *Renewable and Sustainable Energy Reviews*, 157 (2022) 112020.
- 1123 [10] R. Yukesh Kannah, J. Merrylin, T. Poornima Devi, S. Kavitha, P. Sivashanmugam, G. Kumar,
1124 J. Rajesh Banu, Food waste valorization: Biofuels and value added product recovery, *Bioresource*
1125 *Technology Reports*, 11 (2020) 100524.
- 1126 [11] S. Patumsawad, Co-firing of high moisture content MSW with coal in a fluidized bed
1127 combustor, (2000).
- 1128 [12] S. Ajanko, A. Moilanen, J. Juvonen, The effect of wastes. Source separation system and
1129 handling technique on the quality of solid recovered fuel; Jaetteiden
1130 syntypaikkalajittelujaerjestelmaen ja kaesittelytekniikan vaikutus kierraetyspolttoaineen laatuun,
1131 (2005).
- 1132 [13] M. Becidan, L. Sørum, D. Lindberg, Impact of municipal solid waste (MSW) quality on the
1133 behavior of alkali metals and trace elements during combustion: a thermodynamic equilibrium
1134 analysis, *Energy & fuels*, 24 (2010) 3446–3455.
- 1135 [14] J. Zhao, B. Li, X. Wei, Y. Zhang, T. Li, Slagging characteristics caused by alkali and alkaline
1136 earth metals during municipal solid waste and sewage sludge co-incineration, *Energy*, 202 (2020)
1137 117773.
- 1138 [15] W. Ma, G. Hoffmann, M. Schirmer, G. Chen, V.S. Rotter, Chlorine characterization and
1139 thermal behavior in MSW and RDF, *Journal of hazardous materials*, 178 (2010) 489–498.
- 1140 [16] K. Phoungthong, Y. Xia, H. Zhang, L. Shao, P. He, Leaching toxicity characteristics of
1141 municipal solid waste incineration bottom ash, *Frontiers of Environmental Science & Engineering*,
1142 10 (2016) 399–411.
- 1143 [17] L. Su, S. Wang, R. Ji, G. Zhuo, C. Liu, M. Chen, H. Li, L. Zhang, New insight into the role
1144 of FDOM in heavy metal leaching behavior from MSWI bottom ash during accelerated weathering
1145 using fluorescence EEM-PARAFAC, *Waste Management*, 144 (2022) 153–162.

- 1146 [18] W.-C. Kuo, J. Lasek, K. Słowik, K. Głód, B. Jagustyn, Y.-H. Li, A. Cygan, Low-temperature
1147 pre-treatment of municipal solid waste for efficient application in combustion systems, *Energy*
1148 *Conversion and Management*, 196 (2019) 525–535.
- 1149 [19] A. Fazil, S. Kumar, S.M. Mahajani, Gasification and Co-gasification of paper-rich, high-ash
1150 refuse-derived fuel in downdraft gasifier, *Energy*, 263 (2023) 125659.
- 1151 [20] K.A. Abdulyekeen, W.M.A.W. Daud, M.F.A. Patah, F. Abnisa, Torrefaction of municipal
1152 solid waste to enhanced hydrophobic solid fuel: parametric optimisation and optimised torrefied
1153 solid products characterisation, grindability, and pyrolysis behaviour, *Biomass Conversion and*
1154 *Biorefinery*, 14 (2024) 30251–30268.
- 1155 [21] N. Saha, E. Fillerup, B. Thomas, C. Pilgrim, T. Causer, D. Herren, J. Klinger, Improving
1156 bamboo’s fuel and storage properties with a net energy export through torrefaction paired with
1157 catalytic oxidation, *Chemical Engineering Journal*, 440 (2022) 135750.
- 1158 [22] L.A. Ruth, Energy from municipal solid waste: A comparison with coal combustion
1159 technology, *Progress in Energy and Combustion Science*, 24 (1998) 545–564.
- 1160 [23] W.M. Randall Seeker, Waste combustion, Symposium (International) on Combustion, 23
1161 (1991) 867–885.
- 1162 [24] N.J. Themelis, C. Mussche, Municipal solid waste management and waste-to-energy in the
1163 United States, China and Japan, in: 2nd international academic symposium on enhanced landfill
1164 mining, Houthalen-Helchteren, 2013, pp. 14–16.
- 1165 [25] P. Iyer, T. Rao, P. Grover, N. Singh, Biomass thermo-chemical characterization, *Chemical*
1166 *Engineering Department, IIT Delhi*, 45 (2002).
- 1167 [26] C. Lousselet, F. Cherubini, G. del Alamo Serrano, M. Becidan, A.H. Strømman, Life-cycle
1168 assessment of a Waste-to-Energy plant in central Norway: Current situation and effects of changes
1169 in waste fraction composition, *Waste management*, 58 (2016) 191–201.
- 1170 [27] A.W. Larsen, K. Fuglsang, N.H. Pedersen, J. Fellner, H. Rechberger, T. Astrup, Biogenic
1171 carbon in combustible waste: Waste composition, variability and measurement uncertainty, *Waste*
1172 *Management & Research*, 31 (2013) 56–66.
- 1173 [28] S. Chai, R. Zakaria, INVESTIGATION ON COMBUSTION CHARACTERISTICS OF
1174 MUNICIPAL SOLID WASTE FROM PENANG STATE MALAYSIA, (2006).
- 1175 [29] E. Alakangas, M. Hurskainen, J. Laatikainen-Luntama, J. Korhonen, Suomessa käytettävien
1176 polttoaineiden ominaisuuksia, in: Valtion teknillinen tutkimuskeskus, 2000.
- 1177 [30] L. Hietanen, MSW source separation and REF production-experiences, in: VTT
1178 SYMPOSIUM, VTT; 1999, 2002, pp. 243–252.
- 1179 [31] L. Meraz, A. Domínguez, I. Kornhauser, F. Rojas, A thermochemical concept-based equation
1180 to estimate waste combustion enthalpy from elemental composition☆, *Fuel*, 82 (2003) 1499–1507.
- 1181 [32] L. Lu, T. Namioka, K. Yoshikawa, Effects of hydrothermal treatment on characteristics and
1182 combustion behaviors of municipal solid wastes, *Applied Energy*, 88 (2011) 3659–3664.
- 1183 [33] J. Parikh, S. Channiwala, G. Ghosal, A correlation for calculating HHV from proximate
1184 analysis of solid fuels, *Fuel*, 84 (2005) 487–494.
- 1185 [34] R. Amen, J. Hameed, G. Albashar, H.W. Kamran, M.U.H. Shah, M.K.U. Zaman, A. Mukhtar,
1186 S. Saqib, S.I. Ch, M. Ibrahim, Modelling the higher heating value of municipal solid waste for
1187 assessment of waste-to-energy potential: a sustainable case study, *Journal of cleaner production*,
1188 287 (2021) 125575.
- 1189 [35] V. Morcos, Energy recovery from municipal solid waste incineration—A review, *Heat*
1190 *Recovery Systems and CHP*, 9 (1989) 115–126.

- 1191 [36] Z. Xia, P. Shan, C. Chen, H. Du, J. Huang, L. Bai, A two-fluid model simulation of an
1192 industrial moving grate waste incinerator, *Waste Management*, 104 (2020) 183–191.
- 1193 [37] T. Gu, C. Yin, W. Ma, G. Chen, Municipal solid waste incineration in a packed bed: A
1194 comprehensive modeling study with experimental validation, *Applied Energy*, 247 (2019) 127–
1195 139.
- 1196 [38] J. Soria, D. Gauthier, G. Flamant, R. Rodriguez, G. Mazza, Coupling scales for modelling
1197 heavy metal vaporization from municipal solid waste incineration in a fluid bed by CFD, *Waste
1198 Management*, 43 (2015) 176–187.
- 1199 [39] A.C.H. Lai, A.W.-K. Law, Numerical modeling of municipal waste bed incineration,
1200 *International Journal of Numerical Methods for Heat & Fluid Flow*, 29 (2018) 504–522.
- 1201 [40] J. Xie, W. Zhong, Y. Shao, Q. Liu, L. Liu, G. Liu, Simulation of Combustion of Municipal
1202 Solid Waste and Coal in an Industrial-Scale Circulating Fluidized Bed Boiler, *Energy & Fuels*, 31
1203 (2017) 14248–14261.
- 1204 [41] F. Alobaid, W.A.K. Al-Maliki, T. Lanz, M. Haaf, A. Brachthäuser, B. Epple, I. Zorbach,
1205 Dynamic simulation of a municipal solid waste incinerator, *Energy*, 149 (2018) 230–249.
- 1206 [42] I. Shunda, X. Jiang, Y. Zhao, J. Yan, Disposal technology and new progress for dioxins and
1207 heavy metals in fly ash from municipal solid waste incineration: A critical review, *Environmental
1208 Pollution*, 311 (2022) 119878.
- 1209 [43] G. Mazza, Q. Falcoz, D. Gauthier, G. Flamant, A particulate model of solid waste incineration
1210 in a fluidized bed combining combustion and heavy metal vaporization, *Combustion and Flame*,
1211 156 (2009) 2084–2092.
- 1212 [44] Y. Cheng, S. Oleszek, K. Shiota, K. Oshita, M. Takaoka, Comparison of sewage sludge mono-
1213 incinerators: Mass balance and distribution of heavy metals in step grate and fluidized bed
1214 incinerators, *Waste Management*, 105 (2020) 575–585.
- 1215 [45] J. Wang, Y. Xue, X. Zhang, X. Shu, Numerical study of radiation effect on the municipal
1216 solid waste combustion characteristics inside an incinerator, *Waste Management*, 44 (2015) 116–
1217 124.
- 1218 [46] A. McPhail, R. Griffin, M. El-Halwagi, K. Medlock, P.J.J. Alvarez, Environmental,
1219 Economic, and Energy Assessment of the Ultimate Analysis and Moisture Content of Municipal
1220 Solid Waste in a Parallel Co-combustion Process, *Energy & Fuels*, 28 (2014) 1453–1462.
- 1221 [47] X. Zhang, Y. Li, X. Zhang, P. Ma, X. Xing, Co-combustion of municipal solid waste and
1222 hydrochars under non-isothermal conditions: Thermal behaviors, gaseous emissions and kinetic
1223 analyses by TGA–FTIR, *Energy*, 265 (2023) 126373.
- 1224 [48] N. Peng, Z. Liu, T. Liu, C. Gai, Emissions of polycyclic aromatic hydrocarbons (PAHs)
1225 during hydrothermally treated municipal solid waste combustion for energy generation, *Applied
1226 Energy*, 184 (2016) 396–403.
- 1227 [49] I. Boumanchar, Y. Chhiti, F.E. M'Hamdi Alaoui, M. Elkhouchi, A. Sahibed-dine, F. Bentiss,
1228 C. Jama, M. Bensitel, Investigation of (co)-combustion kinetics of biomass, coal and municipal
1229 solid wastes, *Waste Management*, 97 (2019) 10–18.
- 1230 [50] L. Rigamonti, M. Grosso, L. Biganzoli, Environmental assessment of refuse-derived fuel co-
1231 combustion in a coal-fired power plant, *Journal of Industrial Ecology*, 16 (2012) 748–760.
- 1232 [51] Y.P. Rago, F.-X. Collard, J.F. Görgens, D. Surroop, R. Mohee, Co-combustion of torrefied
1233 biomass-plastic waste blends with coal through TGA: Influence of synergistic behaviour, *Energy*,
1234 239 (2022) 121859.
- 1235 [52] H. Wu, L. Zhu, J. Cai, H. Lv, Effect of Sewage Sludge Addition on the Co-Combustion
1236 Characteristics of Municipal Solid Waste Incineration, *Processes*, 12 (2024) 2172.

1237 [53] T. Gu, W. Ma, T. Berning, Z. Guo, R. Andersson, C. Yin, Advanced simulation of a 750 t/d
1238 municipal solid waste grate boiler to better accommodate feedstock changes due to waste
1239 classification, *Energy*, 254 (2022) 124338.

1240 [54] B. Liu, Z. Han, X. Liang, Dioxin emissions from municipal solid waste incineration in the
1241 context of waste classification policy, *Atmospheric Pollution Research*, 14 (2023) 101842.

1242 [55] C. Wen, X. Lin, Y. Ying, Y. Ma, H. Yu, X. Li, J. Yan, Dioxin emission prediction from a
1243 full-scale municipal solid waste incinerator: Deep learning model in time-series input, *Waste
1244 Management*, 170 (2023) 93–102.

1245 [56] Z.T. Yaqub, B.O. Oboirien, H. Leion, Process optimization of chemical looping combustion
1246 of solid waste/biomass using machine learning algorithm, *Renewable Energy*, 225 (2024) 120298.

1247 [57] F. Huber, D. Blasenbauer, P. Aschenbrenner, J. Fellner, Complete determination of the
1248 material composition of municipal solid waste incineration bottom ash, *Waste Management*, 102
1249 (2020) 677–685.

1250 [58] W. Li, D. Yan, L. Li, Z. Wen, M. Liu, S. Lu, Q. Huang, Review of thermal treatments for the
1251 degradation of dioxins in municipal solid waste incineration fly ash: Proposing a suitable method
1252 for large-scale processing, *Science of The Total Environment*, 875 (2023) 162565.

1253 [59] F. Vakilchap, S.M. Mousavi, Structural study and metal speciation assessments of waste
1254 PCBs and environmental implications: Outlooks for choosing efficient recycling routes, *Waste
1255 Management*, 151 (2022) 181–194.

1256 [60] I.-e. Noor, A. Martin, O. Dahl, Water recovery from flue gas condensate in municipal solid
1257 waste fired cogeneration plants using membrane distillation, *Chemical Engineering Journal*, 399
1258 (2020) 125707.

1259 [61] Y. Kalmykova, K. Karlfeldt Fedje, Phosphorus recovery from municipal solid waste
1260 incineration fly ash, *Waste Management*, 33 (2013) 1403–1410.

1261 [62] C.H.K. Lam, A.W.M. Ip, J.P. Barford, G. McKay, Use of Incineration MSW Ash: A Review,
1262 in: *Sustainability*, 2010, pp. 1943–1968.

1263 [63] J.D. Eusden, T.T. Eighmy, K. Hockert, E. Holland, K. Marsella, Petrogenesis of municipal
1264 solid waste combustion bottom ash, *Applied Geochemistry*, 14 (1999) 1073–1091.

1265 [64] A.T. Lima, L.M. Ottosen, A.J. Pedersen, A.B. Ribeiro, Characterization of fly ash from bio
1266 and municipal waste, *Biomass and Bioenergy*, 32 (2008) 277–282.

1267 [65] W. Li, Q. Yu, K. Gu, Y. Sun, Y. Wang, P. Zhang, Z. Zheng, Y. Guo, M. Xin, R. Bian, Stability
1268 evaluation of potentially toxic elements in MSWI fly ash during carbonation in view of two
1269 leaching scenarios, *Science of The Total Environment*, 803 (2022) 150135.

1270 [66] X. Lin, M. Yan, A. Dai, M. Zhan, J. Fu, X. Li, T. Chen, S. Lu, A. Buekens, J. Yan,
1271 Simultaneous suppression of PCDD/F and NO_x during municipal solid waste incineration,
1272 *Chemosphere*, 126 (2015) 60–66.

1273 [67] Y. Tang, X. Ma, Z. Lai, D. Zhou, H. Lin, Y. Chen, NO_x and SO₂ emissions from municipal
1274 solid waste (MSW) combustion in CO₂/O₂ atmosphere, *Energy*, 40 (2012) 300–306.

1275 [68] W.H. Cheung, V.K.C. Lee, G. McKay, Minimizing Dioxin Emissions from Integrated MSW
1276 Thermal Treatment, *Environmental Science & Technology*, 41 (2007) 2001–2007.

1277 [69] H. Zhou, L. Hong, D. Chen, J. Lu, X. Song, Influences of Non-SCR De-NO_x Technologies
1278 on NO_x and Dioxin Emissions in Full Scale Municipal Solid Waste (MSW) Incinerators, *Aerosol
1279 and Air Quality Research*, 24 (2024) 230319.

1280 [70] A.A.M. Rahat, C. Wang, R.M. Everson, J.E. Fieldsend, Data-driven multi-objective
1281 optimisation of coal-fired boiler combustion systems, *Applied Energy*, 229 (2018) 446–458.

1282 [71] N. Tenhumberg, EU Regulatory Compliance of Renewable Fuels from Steel Mill Gases and
1283 Exhaust Gases, *Chemie Ingenieur Technik*, 96 (2024) 1299–1309.

1284 [72] I. Hodgkinson, R. Maletz, F.-G. Simon, C. Dornack, Mini-review of waste-to-energy related
1285 air pollution and their limit value regulations in an international comparison, *Waste Management
1286 & Research*, 40 (2021) 849–858.

1287 [73] M. Kheirnik, S. Ahmed, N. Rahmanian, Comparative techno-economic analysis of carbon
1288 capture processes: Pre-combustion, post-combustion, and oxy-fuel combustion operations,
1289 *Sustainability*, 13 (2021) 13567.

1290 [74] M. Becidan, M. Ditaranto, P. Carlsson, J. Bakken, M.N. Olsen, J. Stuen, Oxyfuel combustion
1291 of a model MSW—an experimental study, *Energies*, 14 (2021) 5297.

1292 [75] C. Fu, M. Ditaranto, M. Becidan, D. Berstad, J. Stuen, Conceptual design and process
1293 assessment of a MSW waste-to-energy plant with oxy-combustion CO₂ capture, *Carbon
1294 Management*, 16 (2025) 2473913.

1295 [76] R.J. Giraud, P.H. Taylor, C.-p. Huang, Combustion operating conditions for municipal Waste-
1296 to-Energy facilities in the U.S, *Waste Management*, 132 (2021) 124–132.

1297 [77] L. Lombardi, E. Carnevale, A. Corti, A review of technologies and performances of thermal
1298 treatment systems for energy recovery from waste, *Waste Management*, 37 (2015) 26–44.

1299 [78] N.L. Panwar, P.R. Lanjekar, K. Soni, Plasma gasification of municipal solid waste: a life
1300 cycle thinking perspective on energy, emissions, and economic feasibility, *Discover Sustainability*,
1301 6 (2025) 1164.

1302 [79] R. Mallick, P. Vairakannu, Plasma gasification as a potential solution for waste minimization
1303 and clean energy production: A critical review on techno-economic-environmental assessment and
1304 modelling approaches, *Waste Management*, 208 (2025) 115158.

1305 [80] U. Azhagu, D. Muniyappan, A. Ramanathan, Advancements in plasma technology for circular
1306 waste management and green hydrogen production: A review, *Journal of Renewable and
1307 Sustainable Energy*, 17 (2025).

1308 [81] M.A. Shaji, F. Eboh, A. Rabinovich, L. Dor, A. Fridman, Plasma-Induced Abatement of Tar
1309 from Syngas Produced in Municipal Waste Gasification: Thermodynamic Modeling with
1310 Experimental Validation, *Plasma*, 8 (2025) 6.

1311 [82] R. Anilkumar, A.K. Vinayak, B. Kiran, A.V. Gurumoorthy, Study of municipal solid waste
1312 treatment using plasma gasification by application of Aspen Plus, *Chemical Product and Process
1313 Modeling*, 19 (2024) 901–915.

1314 [83] G. Xiao, Study on MSW fluidized-bed gasification and melting technology [D], in, Doctoral
1315 Thesis. Zhejiang University, Hangzhou, China, 2006.

1316 [84] B. Wang, R. Gupta, L. Bei, Q. Wan, L. Sun, A review on gasification of municipal solid waste
1317 (MSW): Syngas production, tar formation, mineral transformation and industrial challenges,
1318 *International Journal of Hydrogen Energy*, 48 (2023) 26676–26706.

1319 [85] K. Im-orb, L. Simasatitkul, A. Arpornwichanop, Analysis of synthesis gas production with a
1320 flexible H₂/CO ratio from rice straw gasification, *Fuel*, 164 (2016) 361–373.

1321 [86] Y.N. Chun, S.C. Kim, K. Yoshikawa, Pyrolysis gasification of dried sewage sludge in a
1322 combined screw and rotary kiln gasifier, *Applied Energy*, 88 (2011) 1105–1112.

1323 [87] U. Arena, F. Di Gregorio, Gasification of a solid recovered fuel in a pilot scale fluidized bed
1324 reactor, *Fuel*, 117 (2014) 528–536.

1325 [88] A. Veksha, A. Giannis, G. Yuan, J. Tng, W.P. Chan, V.W.-C. Chang, G. Lisak, T.-T. Lim,
1326 Distribution and modeling of tar compounds produced during downdraft gasification of municipal
1327 solid waste, *Renewable energy*, 136 (2019) 1294–1303.

1328 [89] L. Cao, K. Iris, X. Xiong, D.C. Tsang, S. Zhang, J.H. Clark, C. Hu, Y.H. Ng, J. Shang, Y.S.
1329 Ok, Biorenewable hydrogen production through biomass gasification: A review and future
1330 prospects, *Environmental research*, 186 (2020) 109547.

1331 [90] M. Irfan, A. Li, L. Zhang, M. Javid, M. Wang, S. Khushk, Enhanced H₂ production from
1332 municipal solid waste gasification using Ni–CaO–TiO₂ bifunctional catalyst prepared by dc arc
1333 plasma melting, *Industrial & Engineering Chemistry Research*, 58 (2019) 13408–13419.

1334 [91] X. Zheng, Z. Ying, B. Wang, C. Chen, CO₂ gasification of municipal solid waste in a drop-
1335 tube reactor: experimental study and thermodynamic analysis of syngas, *Energy & Fuels*, 32
1336 (2018) 5302–5312.

1337 [92] Q. Zhang, L. Dor, W. Yang, W. Blasiak, Eulerian model for municipal solid waste gasification
1338 in a fixed-bed plasma gasification melting reactor, *Energy & fuels*, 25 (2011) 4129–4137.

1339 [93] M. Niu, Y. Huang, B. Jin, X. Wang, Simulation of syngas production from municipal solid
1340 waste gasification in a bubbling fluidized bed using Aspen Plus, *Industrial & engineering
1341 chemistry research*, 52 (2013) 14768–14775.

1342 [94] C. Chen, Y.-Q. Jin, J.-H. Yan, Y. Chi, Simulation of municipal solid waste gasification in two
1343 different types of fixed bed reactors, *Fuel*, 103 (2013) 58–63.

1344 [95] O. Tezer, N. Karabag, M.U. Ozturk, A. Ongen, A. Ayol, Comparison of green waste
1345 gasification performance in updraft and downdraft fixed bed gasifiers, *International Journal of
1346 Hydrogen Energy*, 47 (2022) 31864–31876.

1347 [96] A. Jančauskas, N. Striūgas, K. Zakarauskas, R. Skvorčinskienė, J. Eimontas, K. Buinevičius,
1348 Experimental investigation of sorted municipal solid wastes producer gas composition in an
1349 updraft fixed bed gasifier, *Energy*, 289 (2024) 130063.

1350 [97] G. Vonk, B. Piriou, P.F. Dos Santos, D. Wolbert, G. Vaitilingom, Comparative analysis of
1351 wood and solid recovered fuels gasification in a downdraft fixed bed reactor, *Waste Management*,
1352 85 (2019) 106–120.

1353 [98] M.d.P. González-Vázquez, R. García, M. Gil, C. Pevida, F. Rubiera, Comparison of the
1354 gasification performance of multiple biomass types in a bubbling fluidized bed, *Energy
1355 Conversion and Management*, 176 (2018) 309–323.

1356 [99] A. Shehzad, M.J. Bashir, S. Sethupathi, System analysis for synthesis gas (syngas) production
1357 in Pakistan from municipal solid waste gasification using a circulating fluidized bed gasifier,
1358 *Renewable and Sustainable Energy Reviews*, 60 (2016) 1302–1311.

1359 [100] M. Munir, I. Mardon, S. Al-Zuhair, A. Shawabkeh, N. Saqib, Plasma gasification of
1360 municipal solid waste for waste-to-value processing, *Renewable and Sustainable Energy Reviews*,
1361 116 (2019) 109461.

1362 [101] L. Mazzoni, I. Janajreh, S. Elagroudy, Gasification comparison between plasma and
1363 entrained flow: Analysis of the power plant, in: 2018 6th International Renewable and Sustainable
1364 Energy Conference (IRSEC), IEEE, 2018, pp. 1–7.

1365 [102] Q. Zhang, L. Dor, L. Zhang, W. Yang, W. Blasiak, Performance analysis of municipal solid
1366 waste gasification with steam in a Plasma Gasification Melting reactor, *Applied energy*, 98 (2012)
1367 219–229.

1368 [103] W. Gao, M. Farahani, M. Rezaei, S. Hosamani, M. Jamil, M. Imran, A. Baig, Experimental
1369 study of steam-gasification of municipal solid wastes (MSW) using Ni-Cu/ γ -Al₂O₃ nano
1370 catalysts, *Energy Sources, Part A: Recovery, Utilization, and Environmental Effects*, 39 (2017)
1371 693–697.

1372 [104] S. Jeong, T. Lee, S.J. Lim, Y.-K. Park, S. Kim, Y.-M. Kim, In-Situ Catalytic Gasification of
1373 Rice Hull Using Municipal Solid Waste Incineration Bottom Ash, *Journal of Nanoscience and*
1374 *Nanotechnology*, 21 (2021) 3764–3768.

1375 [105] J. You, X. Chen, Y. Huang, Y. Tian, H. Huang, Hydrogen-rich gas production from catalytic
1376 steam-gasification of municipal solid waste (MSW): Product gas upgrading by in-bed use of
1377 olivine, *Journal of the Energy Institute*, (2025) 102221.

1378 [106] S.-S. Kim, J.W. Kim, S.H. Park, S.-C. Jung, J.-K. Jeon, C. Ryu, Y.-K. Park, Catalytic
1379 Gasification of Mandarin Waste Residue using Ni/CeO₂-ZrO₂, *Bulletin of the Korean Chemical*
1380 *Society*, 34 (2013) 3387–3390.

1381 [107] I. Lazzarotto, S. Ferreira, J. Junges, G. Bassanesi, C. Manera, D. Perondi, M. Godinho, The
1382 role of CaO in the steam gasification of plastic wastes recovered from the municipal solid waste
1383 in a fluidized bed reactor, *Process Safety and Environmental Protection*, 140 (2020) 60–67.

1384 [108] Y. Gao, M. Wang, A. Raheem, F. Wang, J. Wei, D. Xu, X. Song, W. Bao, A. Huang, S.
1385 Zhang, Syngas production from biomass gasification: Influences of feedstock properties, reactor
1386 type, and reaction parameters, *ACS omega*, 8 (2023) 31620–31631.

1387 [109] W.P. Chan, A. Veksha, J. Lei, W.-D. Oh, X. Dou, A. Giannis, G. Lisak, T.-T. Lim, A hot
1388 syngas purification system integrated with downdraft gasification of municipal solid waste,
1389 *Applied Energy*, 237 (2019) 227–240.

1390 [110] A.R. Saleh, B. Sudarmanta, H. Fansuri, O. Muraza, Syngas production from municipal solid
1391 waste with a reduced tar yield by three-stages of air inlet to a downdraft gasifier, *Fuel*, 263 (2020)
1392 116509.

1393 [111] A. Saravanakumar, W.-H. Chen, K.D. Arunachalam, Y.-K. Park, H. Chyuan Ong, Pilot-
1394 scale study on downdraft gasification of municipal solid waste with mass and energy balance
1395 analysis, *Fuel*, 315 (2022) 123287.

1396 [112] M. Ouadi, J.G. Brammer, M. Kay, A. Hornung, Fixed bed downdraft gasification of paper
1397 industry wastes, *Applied Energy*, 103 (2013) 692–699.

1398 [113] I. Temaja, I. Winaya, I. Wirawan, M. Sucipta, I. Swamardika, I. Darma, I.d.J. Leite,
1399 Optimizing Syngas Production from Municipal Solid Waste Gasification: A Dual Reactor
1400 Fluidized Bed Study with Steam and CO₂ as Gasification Agents, *J. Adv. Res. Fluid. Mech.*
1401 *Therm. Sci*, 123 (2024) 222–232.

1402 [114] Q. Zhou, Y. Shen, X. Gu, Progress in torrefaction pretreatment for biomass gasification,
1403 *Green Chemistry*, 26 (2024) 9652–9670.

1404 [115] S. Ge, M.H. Tahir, D. Chen, L. Hong, Y. Feng, Z. Huang, MSW pyro-gasification using
1405 high-temperature CO₂ as gasifying agent: Influence of contact mode between CO₂, char and
1406 volatiles on final products, *Waste Management*, 170 (2023) 112–121.

1407 [116] R. Lopes, D. Roberts, The CO₂ gasification reactivity of chars produced from Australian
1408 municipal solid waste, *Fuel*, 185 (2016) 847–854.

1409 [117] A.M. Alsawadi, R. Marsh, J.M. Steer, D. Morgan, A study of the mechanisms associated
1410 with CO₂ utilisation via the reverse Boudouard reaction, *Fuel*, 381 (2025) 133448.

1411 [118] U.H. Kun, E. Ksepko, Advancing Municipal Solid Waste Management Through Gasification
1412 Technology, *Processes*, (2025).

1413 [119] J. Shen, Y. Li, S. Kang, B. Miao, Z. Deng, P. Yao, S. Liu, J. Wang, Z. Zhong, S.H. Chan,
1414 Efficient methanol production by combining municipal solid waste gasification, SOEC and
1415 methanolation reactor: A thermodynamic study, *Energy*, (2025) 137642.

1416 [120] A. Borgogna, A. Salladini, L. Spadacini, A. Pitrelli, M.C. Annesini, G. Iaquaniello,
1417 Methanol production from Refuse Derived Fuel: Influence of feedstock composition on process
1418 yield through gasification analysis, *Journal of Cleaner Production*, 235 (2019) 1080–1089.

1419 [121] J. Qin, Y. Zhang, S. Heberlein, G. Lisak, Y. Yi, Characterization and comparison of
1420 gasification and incineration fly ashes generated from municipal solid waste in Singapore, *Waste
1421 Management*, 146 (2022) 44–52.

1422 [122] J. Marinkovic, M. Seemann, G.L. Schwebel, H. Thunman, Impact of Biomass Ash–Bauxite
1423 Bed Interactions on an Indirect Biomass Gasifier, *Energy & Fuels*, 30 (2016) 4044–4052.

1424 [123] E.-C. Su, R.-C. Fu, C.-L. Lin, Application of modified olivine to a two-stage gasification
1425 process to evaluate the effects on hydrogen generation and retention of heavy metals, *Applied
1426 Thermal Engineering*, 236 (2024) 121665.

1427 [124] H. Braidy, Characterization and reduction of the release of sulfur and chlorine compounds
1428 in pyrolysis and gasification of biomass and waste, in, *Université de Lorraine*, 2023.

1429 [125] J.-S. Lu, Y. Chang, C.-S. Poon, D.-J. Lee, Slow pyrolysis of municipal solid waste (MSW):
1430 A review, *Bioresource Technology*, 312 (2020) 123615.

1431 [126] X. Ming, F. Xu, Y. Jiang, P. Zong, B. Wang, J. Li, Y. Qiao, Y. Tian, Thermal degradation
1432 of food waste by TG-FTIR and Py-GC/MS: Pyrolysis behaviors, products, kinetic and
1433 thermodynamic analysis, *Journal of Cleaner Production*, 244 (2020) 118713.

1434 [127] N. Wang, K. Qian, D. Chen, H. Zhao, L. Yin, Upgrading gas and oil products of the
1435 municipal solid waste pyrolysis process by exploiting in-situ interactions between the volatile
1436 compounds and the char, *Waste Management*, 102 (2020) 380–390.

1437 [128] M. Ayiania, E. Terrell, A. Duns Moor, F.M. Carbajal-Gamarra, M. Garcia-Perez,
1438 Characterization of solid and vapor products from thermochemical conversion of municipal solid
1439 waste woody fractions, *Waste Management*, 84 (2019) 277–285.

1440 [129] M. Azam, S.S. Jahromy, W. Raza, C. Jordan, M. Harasek, F. Winter, Comparison of the
1441 combustion characteristics and kinetic study of coal, municipal solid waste, and refuse-derived
1442 fuel: Model-fitting methods, *Energy Science & Engineering*, 7 (2019) 2646–2657.

1443 [130] J.T. Fox, A.N. Zook, J. Freiss, B. Appel, J. Appel, C. Ozsuer, M. Sarac, Thermal conversion
1444 of blended food production waste and municipal sewage sludge to recoverable products, *Journal
1445 of Cleaner Production*, 220 (2019) 57–64.

1446 [131] I.M. Gandidi, M.D. Susila, A. Mustofa, N.A. Pambudi, Thermal–catalytic cracking of real
1447 MSW into bio-crude oil, *Journal of the Energy Institute*, 91 (2018) 304–310.

1448 [132] R.K. Singh, B. Ruj, A. Sadhukhan, P. Gupta, Impact of fast and slow pyrolysis on the
1449 degradation of mixed plastic waste: Product yield analysis and their characterization, *Journal of
1450 the Energy Institute*, 92 (2019) 1647–1657.

1451 [133] J. Ma, J. Liu, J. Song, T. Tang, Pressurized carbonization of mixed plastics into porous
1452 carbon sheets on magnesium oxide, *RSC advances*, 8 (2018) 2469–2476.

1453 [134] J. Chen, X. Ma, Z. Yu, T. Deng, X. Chen, L. Chen, M. Dai, A study on catalytic co-pyrolysis
1454 of kitchen waste with tire waste over ZSM-5 using TG-FTIR and Py-GC/MS, *Bioresource
1455 Technology*, 289 (2019) 121585.

1456 [135] J. Wang, Z. Zhong, B. Zhang, K. Ding, Z. Xue, A. Deng, R. Ruan, Upgraded bio-oil
1457 production via catalytic fast co-pyrolysis of waste cooking oil and tea residual, *Waste
1458 Management*, 60 (2017) 357–362.

1459 [136] L. Chen, Z. Yu, S. Fang, M. Dai, X. Ma, Co-pyrolysis kinetics and behaviors of kitchen
1460 waste and *Chlorella vulgaris* using thermogravimetric analyzer and fixed bed reactor, *Energy
1461 Conversion and Management*, 165 (2018) 45–52.

1462 [137] Q. Van Nguyen, Y.S. Choi, S.K. Choi, Y.W. Jeong, Y.S. Kwon, Improvement of bio-crude
1463 oil properties via co-pyrolysis of pine sawdust and waste polystyrene foam, *Journal of*
1464 *Environmental Management*, 237 (2019) 24–29.

1465 [138] W.A. Wan Mahari, C.T. Chong, C.K. Cheng, C.L. Lee, K. Hendrata, P.N. Yuh Yek, N.L.
1466 Ma, S.S. Lam, Production of value-added liquid fuel via microwave co-pyrolysis of used frying
1467 oil and plastic waste, *Energy*, 162 (2018) 309–317.

1468 [139] A. Ephraim, D. Pham Minh, D. Lebonnois, C. Peregrina, P. Sharrock, A. Nzihou, Co-
1469 pyrolysis of wood and plastics: Influence of plastic type and content on product yield, gas
1470 composition and quality, *Fuel*, 231 (2018) 110–117.

1471 [140] P. Lu, Q. Huang, A.C. Bourtsalas, Y. Chi, J. Yan, Synergistic effects on char and oil
1472 produced by the co-pyrolysis of pine wood, polyethylene and polyvinyl chloride, *Fuel*, 230 (2018)
1473 359–367.

1474 [141] E. Üresin, I.I. Gülsaç, M.S. Budak, M. Ünsal, K. Özgür Büyüksakallı, P. Aksoy, A. Sayar,
1475 N. Ünlü, O. Okur, Effects of operational parameters on bio-oil production from biomass, *Waste*
1476 *Management & Research*, 37 (2019) 516–529.

1477 [142] A. Krutof, K.A. Hawboldt, Co-pyrolysis of softwood with waste mussel shells: Liquid
1478 analysis, *Fuel*, 254 (2019) 115584.

1479 [143] Y. Li, X. Xing, P. Ma, X. Zhang, Y. Wu, L. Huang, Effect of alkali and alkaline earth metals
1480 on co-pyrolysis characteristics of municipal solid waste and biomass briquettes, *Journal of*
1481 *Thermal Analysis and Calorimetry*, 139 (2020) 489–498.

1482 [144] A.T. Sipra, N. Gao, H. Sarwar, Municipal solid waste (MSW) pyrolysis for bio-fuel
1483 production: A review of effects of MSW components and catalysts, *Fuel processing technology*,
1484 175 (2018) 131–147.

1485 [145] F. Sotoudehnia, A.B. Rabiou, A. Alayat, A.G. McDonald, Characterization of bio-oil and
1486 biochar from pyrolysis of waste corrugated cardboard, *Journal of analytical and applied pyrolysis*,
1487 145 (2020) 104722.

1488 [146] T. Lee, J.-I. Oh, T. Kim, D.C. Tsang, K.-H. Kim, J. Lee, E.E. Kwon, Controlling generation
1489 of benzenes and polycyclic aromatic hydrocarbons in thermolysis of polyvinyl chloride in CO₂,
1490 *Energy Conversion and Management*, 164 (2018) 453–459.

1491 [147] S. Yousef, J. Eimontas, N. Striūgas, M. Tatariants, M.A. Abdelnaby, S. Tuckute, L.
1492 Kliucininkas, A sustainable bioenergy conversion strategy for textile waste with self-catalysts
1493 using mini-pyrolysis plant, *Energy conversion and management*, 196 (2019) 688–704.

1494 [148] J.A. Onwudili, C. Muhammad, P.T. Williams, Influence of catalyst bed temperature and
1495 properties of zeolite catalysts on pyrolysis-catalysis of a simulated mixed plastics sample for the
1496 production of upgraded fuels and chemicals, *Journal of the Energy Institute*, 92 (2019) 1337–1347.

1497 [149] S.M. Al-Salem, Thermal pyrolysis of high density polyethylene (HDPE) in a novel fixed
1498 bed reactor system for the production of high value gasoline range hydrocarbons (HC), *Process*
1499 *Safety and Environmental Protection*, 127 (2019) 171–179.

1500 [150] H. Kadlimatti, B.R. Mohan, M. Saidutta, Bio-oil from microwave assisted pyrolysis of food
1501 waste-optimization using response surface methodology, *Biomass and Bioenergy*, 123 (2019) 25–
1502 33.

1503 [151] C. Setter, F. Silva, M. Assis, C. Ataíde, P. Trugilho, T. Oliveira, Slow pyrolysis of coffee
1504 husk briquettes: Characterization of the solid and liquid fractions, *Fuel*, 261 (2020) 116420.

1505 [152] B.F. Staley, M.A. Barlaz, Composition of municipal solid waste in the United States and
1506 implications for carbon sequestration and methane yield, *Journal of Environmental engineering*,
1507 135 (2009) 901–909.

1508 [153] D. Chen, L. Yin, H. Wang, P. He, Pyrolysis technologies for municipal solid waste: a review,
1509 Waste management, 34 (2014) 2466–2486.

1510 [154] L. Wang, Y. Zhang, L. Song, Experimental research on pyrolysis process of waste rubber,
1511 Liaoning Gongcheng Jishu Daxue Xuebao (Ziran Kexue Ban)/J. Liaoning Tech. Univ.(Natural
1512 Science Edition), 25 (2006) 336–338.

1513 [155] S.-Q. Li, J.-H. Yan, R.-D. Li, Y. Chi, K.-F. Cen, Axial transport and residence time of MSW
1514 in rotary kilns: Part I. Experimental, Powder technology, 126 (2002) 217–227.

1515 [156] X. Dai, X. Yin, C. Wu, W. Zhang, Y. Chen, Pyrolysis of waste tires in a circulating fluidized-
1516 bed reactor, Energy, 26 (2001) 385–399.

1517 [157] J. Aguado, D. Serrano, J. Escola, E. Garagorri, Catalytic conversion of low-density
1518 polyethylene using a continuous screw kiln reactor, Catalysis Today, 75 (2002) 257–262.

1519 [158] E. A. Silveira, B. Santanna Chaves, L. Macedo, G.F. Ghesti, R.B.W. Evaristo, G. Cruz
1520 Lamas, S.M. Luz, T.d.P. Protásio, P. Rousset, A hybrid optimization approach towards energy
1521 recovery from torrefied waste blends, Renewable Energy, 212 (2023) 151–165.

1522 [159] S.K. Thengane, K.S. Kung, A. Gomez-Barea, A.F. Ghoniem, Advances in biomass
1523 torrefaction: Parameters, models, reactors, applications, deployment, and market, Progress in
1524 Energy and Combustion Science, 93 (2022) 101040.

1525 [160] K.N. Dhanavath, S. Bankupalli, S.K. Bhargava, R. Parthasarathy, An experimental study to
1526 investigate the effect of torrefaction temperature on the kinetics of gas generation, Journal of
1527 Environmental Chemical Engineering, 6 (2018) 3332–3341.

1528 [161] T.R. Sarker, S. Nanda, V. Meda, A.K. Dalai, Process optimization and investigating the
1529 effects of torrefaction and pelletization on steam gasification of canola residue, Fuel, 323 (2022)
1530 124239.

1531 [162] J. Klinger, E. Bar-Ziv, D. Shonnard, Predicting Properties of Torrefied Biomass by Intrinsic
1532 Kinetics, Energy & Fuels, 29 (2015) 171–176.

1533 [163] T.R. Sarker, R. Azargohar, J. Stobbs, C. Karunakaran, V. Meda, A.K. Dalai, Complementary
1534 effects of torrefaction and pelletization for the production of fuel pellets from agricultural residues:
1535 A comparative study, Industrial Crops and Products, 181 (2022) 114740.

1536 [164] W.-H. Chen, B.-J. Lin, Y.-Y. Lin, Y.-S. Chu, A.T. Ubando, P.L. Show, H.C. Ong, J.-S.
1537 Chang, S.-H. Ho, A.B. Culaba, A. Pétrissans, M. Pétrissans, Progress in biomass torrefaction:
1538 Principles, applications and challenges, Progress in Energy and Combustion Science, 82 (2021)
1539 100887.

1540 [165] M.A. Sukiran, W.M.A. Wan Daud, F. Abnisa, A.B. Nasrin, A.A. Astimar, S.K. Loh,
1541 Individual torrefaction parameter enhances characteristics of torrefied empty fruit bunches,
1542 Biomass Conversion and Biorefinery, 11 (2021) 461–472.

1543 [166] J. Klinger, E. Bar-Ziv, D. Shonnard, Kinetic study of aspen during torrefaction, Journal of
1544 Analytical and Applied Pyrolysis, 104 (2013) 146–152.

1545 [167] H. Yuan, Y. Wang, N. Kobayashi, D. Zhao, S. Xing, Study of Fuel Properties of Torrefied
1546 Municipal Solid Waste, Energy & Fuels, 29 (2015) 4976–4980.

1547 [168] J. Yu, L. Sun, B. Wang, Y. Qiao, J. Xiang, S. Hu, H. Yao, Study on the behavior of heavy
1548 metals during thermal treatment of municipal solid waste (MSW) components, Environmental
1549 Science and Pollution Research, 23 (2016) 253–265.

1550 [169] A. Dawei, W. Zhimin, Z. Shuting, Y. Hongxing, Low-temperature pyrolysis of municipal
1551 solid waste: influence of pyrolysis temperature on the characteristics of solid fuel, International
1552 Journal of Energy Research, 30 (2006) 349–357.

1553 [170] K.L. Iroba, O.-D. Baik, L.G. Tabil, Torrefaction of biomass from municipal solid waste
1554 fractions I: Temperature profiles, moisture content, energy consumption, mass yield, and
1555 thermochemical properties, *Biomass and Bioenergy*, 105 (2017) 320–330.

1556 [171] M. Ivanovski, D. Goričanec, D. Urbančl, The thermochemical conversion of municipal solid
1557 waste by torrefaction process, *Thermo*, 3 (2023) 277–288.

1558 [172] Q. Gao, M. Edo, S.H. Larsson, E. Collina, M. Rudolfsson, M. Gallina, I. Oluwoye, M.
1559 Altarawneh, B.Z. Długogorski, S. Jansson, Formation of PCDDs and PCDFs in the torrefaction of
1560 biomass with different chemical composition, *Journal of Analytical and Applied Pyrolysis*, 123
1561 (2017) 126–133.

1562 [173] Y. Niu, Y. Lv, Y. Lei, S. Liu, Y. Liang, D. Wang, S.e. Hui, Biomass torrefaction: properties,
1563 applications, challenges, and economy, *Renewable and Sustainable Energy Reviews*, 115 (2019)
1564 109395.

1565 [174] K. Głód, J.A. Lasek, K. Supernok, P. Pawłowski, R. Fryza, J. Zuwała, Torrefaction as a way
1566 to increase the waste energy potential, *Energy*, 285 (2023) 128606.

1567 [175] H. Haykiri-Acma, S. Yaman, Effects of torrefaction after pelleting (TAP) process on strength
1568 and fuel characteristics of binderless bio-pellets, *Biomass Conversion and Biorefinery*, 14 (2024)
1569 3489–3500.

1570 [176] S. Zinchik, Z. Xu, S.S. Kolapkar, E. Bar-Ziv, A.G. McDonald, Properties of pellets of
1571 torrefied U.S. waste blends, *Waste Management*, 104 (2020) 130–138.

1572 [177] K.A. Abdulyekeen, W.M.A.W. Daud, M.F.A. Patah, Torrefaction of wood and garden
1573 wastes from municipal solid waste to enhanced solid fuel using helical screw rotation-induced
1574 fluidised bed reactor: Effect of particle size, helical screw speed and temperature, *Energy*, 293
1575 (2024) 130759.

1576 [178] S. Riaz, Y.M. Al-Abdeli, I. Oluwoye, M. Altarawneh, Torrefaction of Densified Woody
1577 Biomass: The Effect of Pellet Size on Thermochemical and Thermophysical Characteristics,
1578 *BioEnergy Research*, 15 (2022) 544–558.

1579 [179] M. Tymoszuik, Investigations of torrefied biomass grindability using a modified Hardgrove
1580 test, in: *E3S Web of Conferences*, EDP Sciences, 2017, pp. 02022.

1581 [180] M. Tymoszuik, J. Wnorowska, S. Kalisz, Grindability Features of Torrefied Biomass,
1582 *Energies*, 18 (2025) 1824.

1583 [181] J.H.A. Khalsa, D. Leistner, N. Weller, L.I. Darvell, B. Dooley, Torrefied biomass pellets—
1584 Comparing grindability in different laboratory mills, *Energies*, 9 (2016) 794.

1585 [182] L. Wang, L. Riva, Ø. Skreiberg, R. Khalil, P. Bartocci, Q. Yang, H. Yang, X. Wang, D.
1586 Chen, M. Rudolfsson, Effect of torrefaction on properties of pellets produced from woody
1587 biomass, *Energy & Fuels*, 34 (2020) 15343–15354.

1588 [183] Z. Smith, B. Isaac, J.S. Tumuluru, N. Yancey, Grinding and pelleting characteristics of
1589 municipal solid waste fractions, *Energies*, 17 (2023) 29.

1590 [184] A. Škorjanc, S. Gruber, K. Rola, D. Goričanec, D. Urbančl, Advancing energy recovery:
1591 evaluating torrefaction temperature effects on food waste properties from fruit and vegetable
1592 processing, *Processes*, 13 (2025) 208.

1593 [185] C.K. Banaget, G.R. Check, I. Watson, Torrefaction of plastics and food waste for biofuel
1594 production, in: *IOP Conference Series: Earth and Environmental Science*, IOP Publishing, 2023,
1595 pp. 012009.

1596 [186] A. Hanoğlu, A. Çay, J. Yanık, Production of biochars from textile fibres through torrefaction
1597 and their characterisation, *Energy*, 166 (2019) 664–673.

1598 [187] R. Jaideep, W.H. Lo, G.P. Lim, C.X. Chua, S. Gan, L.Y. Lee, S. Thangalazhy-Gopakumar,
1599 Enhancement of fuel properties of yard waste through dry torrefaction, *Materials Science for*
1600 *Energy Technologies*, 4 (2021) 156–165.

1601 [188] Y.P. Rago, F.-X. Collard, J.F. Görgens, D. Surroop, R. Mohee, Torrefaction of biomass and
1602 plastic from municipal solid waste streams and their blends: Evaluation of interactive effects, *Fuel*,
1603 277 (2020) 118089.

1604 [189] N. Saha, J. Klinger, E. Fillerup, L. Williams, R. Emerson, D. Hartley, T.A. Barckholtz, G.
1605 Pilloni, Synergistic torrefaction of plastic polymers and biomass, *Energy Conversion and*
1606 *Management*, 341 (2025) 120044.

1607 [190] X. Zhu, S. Li, J. Li, S. Zhou, B. Yan, Y. Sun, G. Chen, A component synergy of flue gas
1608 torrefaction of municipal solid waste, *Fuel Processing Technology*, 238 (2022) 107517.

1609 [191] T.O. Olugbade, O.T. Ojo, Biomass torrefaction for the production of high-grade solid
1610 biofuels: a review, *BioEnergy Research*, 13 (2020) 999–1015.

1611 [192] C. He, C. Tang, C. Li, J. Yuan, K.-Q. Tran, Q.-V. Bach, R. Qiu, Y. Yang, Wet torrefaction
1612 of biomass for high quality solid fuel production: A review, *Renewable and Sustainable Energy*
1613 *Reviews*, 91 (2018) 259–271.

1614 [193] P. Piersa, H. Unyay, S. Szufa, W. Lewandowska, R. Modrzewski, R. Ślęzak, S. Ledakowicz,
1615 An extensive review and comparison of modern biomass torrefaction reactors vs. biomass
1616 pyrolysis—part 1, *Energies*, 15 (2022) 2227.

1617 [194] Q.-V. Bach, Ø. Skreiberg, Upgrading biomass fuels via wet torrefaction: A review and
1618 comparison with dry torrefaction, *Renewable and Sustainable Energy Reviews*, 54 (2016) 665–
1619 677.

1620 [195] L. Dai, Y. Wang, Y. Liu, R. Ruan, C. He, Z. Yu, L. Jiang, Z. Zeng, X. Tian, Integrated
1621 process of lignocellulosic biomass torrefaction and pyrolysis for upgrading bio-oil production: A
1622 state-of-the-art review, *Renewable and Sustainable Energy Reviews*, 107 (2019) 20–36.

1623 [196] K. Moscicki, L. Niedzwiecki, P. Owczarek, M. Wnukowski, Commoditization of wet and
1624 high ash biomass: wet torrefaction—a review, *Power Technol*, 97 (2017) 354–369.

1625 [197] C.M.S. da Silva, A.d.C.O. Carneiro, B.R. Vital, C.G. Figueiró, L. de Freitas Fialho, M.A. de
1626 Magalhães, A.G. Carvalho, W.L. Cândido, Biomass torrefaction for energy purposes—Definitions
1627 and an overview of challenges and opportunities in Brazil, *Renewable and Sustainable Energy*
1628 *Reviews*, 82 (2018) 2426–2432.

1629 [198] S.-Y. Han, C.-W. Park, G.-J. Kwon, N.-H. Kim, J.-C. Kim, S.-H. Lee, Ionic liquid
1630 pretreatment of lignocellulosic biomass, (2020).

1631 [199] Z. Huang, L. Shi, Y. Muhammad, L. Li, Effect of ionic liquid assisted hydrothermal
1632 carbonization on the properties and gasification reactivity of hydrochar derived from eucalyptus,
1633 *Journal of Colloid and Interface Science*, 586 (2021) 423–432.

1634 [200] B. Roy, P. Kleine-Möllhoff, A. Dalibard, Superheated steam Torrefaction of biomass
1635 residues with valorisation of platform chemicals part—2: Economic assessment and
1636 commercialisation opportunities, *Sustainability*, 14 (2022) 2338.

1637 [201] J.L. Klinger, T.L. Westover, R.M. Emerson, C.L. Williams, S. Hernandez, G.D. Monson,
1638 J.C. Ryan, Effect of biomass type, heating rate, and sample size on microwave-enhanced fast
1639 pyrolysis product yields and qualities, *Applied Energy*, 228 (2018) 535–545.

1640 [202] N. Saha, M.T. Reza, Upcycling simulated food wastes into superactivated hydrochar for
1641 remarkable hydrogen storage, *Journal of Analytical and Applied Pyrolysis*, 159 (2021) 105322.

1642 [203] N. Saha, A. Saba, P. Saha, K. McGaughy, D. Franqui-Villanueva, W.J. Orts, W.M. Hart-
1643 Cooper, M.T. Reza, Hydrothermal carbonization of various paper mill sludges: An observation of
1644 solid fuel properties, *Energies*, 12 (2019) 858.

1645 [204] N. Saha, M. Volpe, L. Fiori, R. Volpe, A. Messineo, M.T. Reza, Cationic dye adsorption on
1646 hydrochars of winery and citrus juice industries residues: Performance, mechanism, and
1647 thermodynamics, *Energies*, 13 (2020) 4686.

1648 [205] M.T. Reza, J. Andert, B. Wirth, D. Busch, J. Pielert, J.G. Lynam, J. Mumme, Hydrothermal
1649 carbonization of biomass for energy and crop production, *Appl. Bioenergy*, 1 (2014) 11–29.

1650 [206] S.K. Hoekman, A. Broch, C. Robbins, Hydrothermal carbonization (HTC) of lignocellulosic
1651 biomass, *Energy & Fuels*, 25 (2011) 1802–1810.

1652 [207] A. Toptas Tag, G. Duman, J. Yanik, Influences of feedstock type and process variables on
1653 hydrochar properties, *Bioresource Technology*, 250 (2018) 337–344.

1654 [208] R. Wang, J. Jia, Q. Jin, H. Chen, H. Liu, Q. Yin, Z. Zhao, Forming mechanism of coke
1655 microparticles from polymerization of aqueous organics during hydrothermal carbonization
1656 process of biomass, *Carbon*, 192 (2022) 50–60.

1657 [209] X. Lu, B. Jordan, N.D. Berge, Thermal conversion of municipal solid waste via hydrothermal
1658 carbonization: Comparison of carbonization products to products from current waste management
1659 techniques, *Waste Management*, 32 (2012) 1353–1365.

1660 [210] H. Zhan, S. Zhang, Y. Song, G. Chang, X. Wang, Z. Zeng, Hydrothermal co-carbonization
1661 of industrial biowastes with lignite toward modified hydrochar production: Synergistic effects and
1662 structural characteristics, *Journal of Environmental Chemical Engineering*, 10 (2022) 107540.

1663 [211] M.-M. Titirici, R.J. White, C. Falco, M. Sevilla, Black perspectives for a green future:
1664 hydrothermal carbons for environment protection and energy storage, *Energy & Environmental
1665 Science*, 5 (2012) 6796–6822.

1666 [212] M. Lucian, M. Volpe, L. Gao, G. Piro, J.L. Goldfarb, L. Fiori, Impact of hydrothermal
1667 carbonization conditions on the formation of hydrochars and secondary chars from the organic
1668 fraction of municipal solid waste, *Fuel*, 233 (2018) 257–268.

1669 [213] M.A. Abdoli, R. Ghasemzadeh, Evaluation and optimization of hydrothermal carbonization
1670 condition for hydrochar and methane yield from anaerobic digestion of organic fraction of
1671 municipal solid waste (OFMSW), *Fuel*, 355 (2024) 129531.

1672 [214] M. Lucian, M. Volpe, F. Merzari, D. Wüst, A. Kruse, G. Andreottola, L. Fiori, Hydrothermal
1673 carbonization coupled with anaerobic digestion for the valorization of the organic fraction of
1674 municipal solid waste, *Bioresource Technology*, 314 (2020) 123734.

1675 [215] Y. Lin, X. Ma, X. Peng, Z. Yu, Hydrothermal carbonization of typical components of
1676 municipal solid waste for deriving hydrochars and their combustion behavior, *Bioresource
1677 Technology*, 243 (2017) 539–547.

1678 [216] S. Shekoohiyan, A. Sajadi, G. Moussavi, M. Heidari, Hydrothermal carbonization of plastic
1679 wastes and effect of influential parameters on performance and challenges: a review, *International
1680 Journal of Environmental Science and Technology*, 22 (2025) 8335–8376.

1681 [217] G. Mannarino, S. Caffaz, R. Gori, L. Lombardi, Environmental Life Cycle Assessment of
1682 Hydrothermal Carbonization of Sewage Sludge and Its Products Valorization Pathways, *Waste
1683 and Biomass Valorization*, 13 (2022) 3845–3864.

1684 [218] J.D. Marin-Batista, J.A. Villamil, J.J. Rodriguez, A.F. Mohedano, M.A. de la Rubia,
1685 Valorization of microalgal biomass by hydrothermal carbonization and anaerobic digestion,
1686 *Bioresource Technology*, 274 (2019) 395–402.

1687 [219] C.I. Aragón-Briceño, O. Grasham, A.B. Ross, V. Dupont, M.A. Camargo-Valero,
1688 Hydrothermal carbonization of sewage digestate at wastewater treatment works: Influence of solid
1689 loading on characteristics of hydrochar, process water and plant energetics, *Renewable Energy*,
1690 157 (2020) 959–973.

1691 [220] F. Di Maria, A. Sordi, C. Micale, Optimization of Solid State Anaerobic Digestion by
1692 inoculum recirculation: The case of an existing Mechanical Biological Treatment plant, *Applied*
1693 *Energy*, 97 (2012) 462–469.

1694 [221] S.E. Borglin, T.C. Hazen, C.M. Oldenburg, P.T. Zawislanski, Comparison of aerobic and
1695 anaerobic biotreatment of municipal solid waste, *Journal of the Air & Waste Management*
1696 *Association*, 54 (2004) 815–822.

1697 [222] H.B. Sharma, S. Panigrahi, A.K. Sarmah, B.K. Dubey, Downstream augmentation of
1698 hydrothermal carbonization with anaerobic digestion for integrated biogas and hydrochar
1699 production from the organic fraction of municipal solid waste: A circular economy concept,
1700 *Science of The Total Environment*, 706 (2020) 135907.

1701 [223] M.T. Reza, C. Coronella, K.M. Holtman, D. Franqui-Villanueva, S.R. Poulson,
1702 Hydrothermal Carbonization of Autoclaved Municipal Solid Waste Pulp and Anaerobically
1703 Treated Pulp Digestate, *ACS Sustainable Chemistry & Engineering*, 4 (2016) 3649–3658.

1704 [224] Y. Jin, L. Lu, X. Ma, H. Liu, Y. Chi, K. Yoshikawa, Effects of blending hydrothermally
1705 treated municipal solid waste with coal on co-combustion characteristics in a lab-scale fluidized
1706 bed reactor, *Applied Energy*, 102 (2013) 563–570.

1707 [225] N.D. Berge, K.S. Ro, J. Mao, J.R.V. Flora, M.A. Chappell, S. Bae, Hydrothermal
1708 Carbonization of Municipal Waste Streams, *Environmental Science & Technology*, 45 (2011)
1709 5696–5703.

1710 [226] J. Wei, Q. Guo, L. Ding, K. Yoshikawa, G. Yu, Synergy mechanism analysis of petroleum
1711 coke and municipal solid waste (MSW)-derived hydrochar co-gasification, *Applied Energy*, 206
1712 (2017) 1354–1363.

1713 [227] B. Triyono, P. Prawisudha, M. Aziz, Mardiyati, A.D. Pasek, K. Yoshikawa, Utilization of
1714 mixed organic-plastic municipal solid waste as renewable solid fuel employing wet torrefaction,
1715 *Waste Management*, 95 (2019) 1–9.

1716 [228] Y. Lin, X. Ma, X. Peng, Z. Yu, S. Fang, Y. Lin, Y. Fan, Combustion, pyrolysis and char
1717 CO₂-gasification characteristics of hydrothermal carbonization solid fuel from municipal solid
1718 wastes, *Fuel*, 181 (2016) 905–915.

1719 [229] G. Ischia, L. Fiori, L. Gao, J.L. Goldfarb, Valorizing municipal solid waste via integrating
1720 hydrothermal carbonization and downstream extraction for biofuel production, *Journal of Cleaner*
1721 *Production*, 289 (2021) 125781.

1722 [230] M.T. Islam, A.I. Sultana, N. Saha, J.L. Klinger, M.T. Reza, Pretreatment of Biomass by
1723 Selected Type-III Deep Eutectic Solvents and Evaluation of the Pretreatment Effects on
1724 Hydrothermal Carbonization, *Industrial & Engineering Chemistry Research*, 60 (2021) 15479–
1725 15491.

1726 [231] S. Fakudze, J. Chen, A critical review on co-hydrothermal carbonization of biomass and
1727 fossil-based feedstocks for cleaner solid fuel production: Synergistic effects and environmental
1728 benefits, *Chemical Engineering Journal*, 457 (2023) 141004.

1729 [232] B. Patel, M. Guo, A. Izadpanah, N. Shah, K. Hellgardt, A review on hydrothermal pre-
1730 treatment technologies and environmental profiles of algal biomass processing, *Bioresource*
1731 *Technology*, 199 (2016) 288–299.

1732 [233] Z.-X. Xu, H. Song, P.-J. Li, Z.-X. He, Q. Wang, K. Wang, P.-G. Duan, Hydrothermal
1733 carbonization of sewage sludge: Effect of aqueous phase recycling, *Chemical Engineering Journal*,
1734 387 (2020) 123410.

1735 [234] R.K. Mishra, V. kumar, P. Kumar, K. Mohanty, Hydrothermal liquefaction of biomass for
1736 bio-crude production: A review on feedstocks, chemical compositions, operating parameters,
1737 reaction kinetics, techno-economic study, and life cycle assessment, *Fuel*, 316 (2022) 123377.

1738 [235] B. De Caprariis, P. De Filippis, A. Petrullo, M. Scarsella, Hydrothermal liquefaction of
1739 biomass: Influence of temperature and biomass composition on the bio-oil production, *Fuel*, 208
1740 (2017) 618–625.

1741 [236] T.H. Seehar, S.S. Toor, K. Sharma, A.H. Nielsen, T.H. Pedersen, L.A. Rosendahl, Influence
1742 of process conditions on hydrothermal liquefaction of eucalyptus biomass for biocrude production
1743 and investigation of the inorganics distribution, *Sustainable Energy & Fuels*, 5 (2021) 1477–1487.

1744 [237] K.F. Tzanetis, J.A. Posada, A. Ramirez, Analysis of biomass hydrothermal liquefaction and
1745 biocrude-oil upgrading for renewable jet fuel production: The impact of reaction conditions on
1746 production costs and GHG emissions performance, *Renewable Energy*, 113 (2017) 1388–1398.

1747 [238] H.O. LeClerc, R. Atwi, S.F. Niles, A.M. McKenna, M.T. Timko, R.H. West, A.R. Teixeira,
1748 Elucidating the role of reactive nitrogen intermediates in hetero-cyclization during hydrothermal
1749 liquefaction of food waste, *Green Chemistry*, 24 (2022) 5125–5141.

1750 [239] R. Katakajwala, H. Kopperi, S. Kumar, S. Venkata Mohan, Hydrothermal liquefaction of
1751 biogenic municipal solid waste under reduced H₂ atmosphere in biorefinery format, *Bioresource
1752 Technology*, 310 (2020) 123369.

1753 [240] F. Ahmad, T.R.K.C. Doddapaneni, S.S. Toor, T. Kikas, Reaction mechanism and kinetics
1754 of hydrothermal liquefaction at sub-and supercritical conditions: a review, *Biomass*, 5 (2025) 9.

1755 [241] R. Bao, S. Wang, J. Feng, Y. Duan, K. Liu, J. Zhao, H. Liu, J. Yang, A Review of
1756 Hydrothermal Biomass Liquefaction: Operating Parameters, Reaction Mechanism, and Bio-Oil
1757 Yields and Compositions, *Energy & Fuels*, 38 (2024) 8437–8459.

1758 [242] D.R. Vardon, B. Sharma, J. Scott, G. Yu, Z. Wang, L. Schideman, Y. Zhang, T.J.
1759 Strathmann, Chemical properties of biocrude oil from the hydrothermal liquefaction of *Spirulina*
1760 algae, swine manure, and digested anaerobic sludge, *Bioresource technology*, 102 (2011) 8295–
1761 8303.

1762 [243] O.V. Okoro, Z. Sun, The characterisation of biochar and biocrude products of the
1763 hydrothermal liquefaction of raw digestate biomass, *Biomass Conversion and Biorefinery*, 11
1764 (2021) 2947–2961.

1765 [244] K. Kohansal, S. Toor, K. Sharma, R. Chand, L. Rosendahl, T.H. Pedersen, Hydrothermal
1766 liquefaction of pre-treated municipal solid waste (biopulp) with recirculation of concentrated
1767 aqueous phase, *Biomass and Bioenergy*, 148 (2021) 106032.

1768 [245] S.I. Hussain Shah, T.H. Seehar, M. Raashid, R. Nawaz, Z. Masood, S. Mukhtar, T.A. Al
1769 Johani, A. Doyle, M.N. Bashir, M.M. Ali, M.A. Kalam, Biocrude from hydrothermal liquefaction
1770 of indigenous municipal solid waste for green energy generation and contribution towards circular
1771 economy: A case study of urban Pakistan, *Heliyon*, 10 (2024).

1772 [246] V. Mahadevan, N. Subbaiyan, G. Kannappan Panchamoorthy, A. Jayaseelan, S.K.
1773 Palaniappan, S. Siengchin, Hydrothermal liquefaction of confused waste to bio-oil: A study on
1774 elemental and energy recovery, *Energy Conversion and Management*, 325 (2025) 119353.

1775 [247] Z. Chen, G. Yu, Y. Wang, X. Wang, Fate of heavy metals during co-disposal of municipal
1776 solid waste incineration fly ash and sewage sludge by hydrothermal coupling pyrolysis process,
1777 *Waste Management*, 109 (2020) 28–37.

1778 [248] A. Sánchez-Bayo, R. Rodríguez, V. Morales, N. Nasirian, L.F. Bautista, G. Vicente,
1779 Hydrothermal liquefaction of microalga using metal oxide catalyst, *Processes*, 8 (2019) 15.
1780 [249] T. Yang, C. Du, B. Li, Z. Liu, X. Kai, Influence of alkali and alkaline earth metals on the
1781 hydrothermal liquefaction of lignocellulosic model compounds, *Renewable Energy*, 188 (2022)
1782 1038–1048.
1783 [250] Z. Huang, K. Liu, J. Duan, Q. Wang, A review of waste-containing building materials:
1784 Characterization of the heavy metal, *Construction and Building Materials*, 309 (2021) 125107.
1785 [251] A. Matayeva, S.R. Rasmussen, P. Biller, Distribution of nutrients and phosphorus recovery
1786 in hydrothermal liquefaction of waste streams, *Biomass and Bioenergy*, 156 (2022) 106323.
1787 [252] B. Patel, M. Guo, C. Chong, S.H.M. Sarudin, K. Hellgardt, Hydrothermal upgrading of algae
1788 paste: Inorganics and recycling potential in the aqueous phase, *Science of The Total Environment*,
1789 568 (2016) 489–497.
1790 [253] O. Okoligwe, T. Radu, M.C. Leaper, J.L. Wagner, Characterization of municipal solid waste
1791 residues for hydrothermal liquefaction into liquid transportation fuels, *Waste Management*, 140
1792 (2022) 133–142.
1793 [254] D. Mahesh, S. Ahmad, R. Kumar, S. Chakravarthy, R. Vinu, Hydrothermal liquefaction of
1794 municipal solid wastes for high quality bio-crude production using glycerol as co-solvent,
1795 *Bioresource technology*, 339 (2021) 125537.

1796